Exposure to compound climate hazards transmitted via global agricultural trade networks

Patrick W. Keys[1,*], Elizabeth A. Barnes[1], Noah S. Diffenbaugh[2], Thomas W. Hertel[3], Uris L.C. Baldos[3], and Johanna Hedlund[4]

[1] Department of Atmospheric Science, Colorado State University
[2] Doerr School of Sustainability, Stanford University
[3] Department of Agricultural Economics, Purdue University
[4] Stockholm Environment Institute, Stockholm, Sweden

Acknowledgments
None.

Author contributions
PWK, EAB, and NSD conceived the study; All authors designed the analysis; EAB and ULCB developed the data and code; PWK, EAB, and ULCB conducted the analysis; PWK led the writing of the paper, and all authors contributed to writing the paper.

Conflict of Interest
None.

Data Availability and Code Availability
Code is available on GitHub at https://github.com/eabarnes1010/trade_timelines_public and the code and data will be given a permanent DOI via Zenodo upon publication.

Funding: PWK was supported by USDA-NIFA Award # 2023-67021-39829 (AI-CLIMATE). EAB was supported by NSF Award #AGS-2210068 and with special thanks to David Wallerstein. NSD was supported by Stanford University. TWH was supported by NSF Awards: #2020635 (AccelNet), #1855937 (INFEWS) and # 2118329 (I-GUIDE), as well as support from USDA‐NIFA Hatch project 1003642. JH acknowledges funding from the Knut and Alice Wallenberg Foundation, under grant # 2021.0336.

Abstract

Compound climate hazards, such as co-occurring temperature and precipitation extremes, substantially impact people and ecosystems. Internal climate variability combines with the forced global warming response to determine both the magnitude and spatial distribution of these events, and their consequences can propagate from one country to another via many pathways. We examine how exposure to compound climate hazards in one country is transmitted internationally via agricultural trade networks by analyzing a large ensemble of climate model simulations and comprehensive trade data of four crops (i.e. wheat, maize, rice and soya). Combinations of variability-driven climate patterns and existing global agricultural trade give rise to a wide range of possible outcomes in the current climate. In the most extreme simulated year, 20% or more of the caloric supply in nearly one third of the world's countries are exposed to compound heat and precipitation hazards. Countries with low levels of diversification, both in the number of suppliers and the regional climates of those suppliers, are more likely to import higher fractions of calories (up to 93%) that are exposed to these compound hazards. Understanding how calories exposed to climate hazards are transmitted through agricultural trade networks in the current climate can contribute to improved anticipatory capacity for national governments, international trade policy, and agricultural-sector resilience. We recommend concerted effort be made toward merging cutting-edge seasonal-to-decadal climate prediction with international trade analysis in support of a new era of anticipatory Anthropocene risk management.

Introduction

Climate hazards substantially impact people and ecosystems (Hoeppe 2016). For example, extreme temperatures can cause heat stress and mortality (Ebi *et al* 2021) and collapse agricultural yields (Schlenker and Roberts 2009). Meanwhile, extreme precipitation can cause destructive flooding that leads to substantial mortality and economic harm (Merz *et al* 2021). Compound climate hazards can be even more disastrous as the combination of moderately severe extremes of multiple climate variables can combine to create catastrophic consequences (AghaKouchak *et al* 2020, Field *et al* 2012, Singh *et al* 2023).

In the case of agriculture, combinations of both hot and dry conditions and hot and wet conditions can lead to substantial reductions in cereal crop yields (Lesk *et al* 2022, Haqiqi *et al* 2021). Generally speaking, anomalously high temperatures combined with drier conditions can cause plant stunting and plant mortality, leading to reduced quality and quantity of crop yields (Heino *et al* 2023). While more varied across crop types, the consequences of anomalously high temperatures combined with wet conditions can cause waterlogging of soils, soil compaction, inhibition of plant metabolism, and delayed or inhibited growth (Li *et al* 2019, Parent *et al* 2008, Urban *et al* 2015). For rice specifically, hot-and-wet extremes can lead to degraded plant protein content and reduced plant growth (Lee *et al* 2013), as well as cause quantifiably harmful working conditions for the agricultural workforce (Diaz *et al* 2023, Vecellio *et al* 2023, Hertel and de Lima 2020, De Lima *et al* 2021).

Compound climate hazards can be experienced acutely in physically tele-connected ways around the planet (Mondal *et al* 2023), and their impacts can, in turn, rapidly propagate via networks of international trade to affect other locations (Hedlund *et al* 2018). The notion of environmentally-driven crises propagating from one country to another has been explored in the context of water stress, especially for countries which rely on imports from acutely water-stressed trade partners (Carter *et al* 2021, Ercin *et al* 2021, Challinor *et al* 2017, Dalin *et al* 2012). In addition, international trade has been proposed to mitigate food insecurity issues (Baldos and Hertel 2015). However, much of the work on how the impacts of climate-related hazards may be transmitted via global trade has explored the potential longer-term impacts of climate change on agricultural production and international trade (Hedlund *et al* 2022), often focusing on the global warming trend across many climate model simulations (Verma *et al* 2014).

However, year-to-year variability internal to the climate system itself drives large regional variations in environmental conditions, including compound hazards, that can potentially impact the trade of climate-sensitive crops (Dingel *et al* 2019, Anderson *et al* 2023). In addition,

regional-to-planetary scale phenomena (e.g., El Niño Southern Oscillation, the Pacific Decadal Oscillation, or the North Atlantic Oscillation) (Singh *et al* 2022) can drive tele-connected climate hazards across different regions under the current climate. Thus, while there is substantial evidence that future global warming is likely to increase the frequency of compound climate hazards (Zscheischler and Seneviratne 2017, Zscheischler *et al* 2018, 2022, Bevacqua *et al* 2023, AghaKouchak *et al* 2020, Ridder *et al* 2022), internal climate variability coupled with existing trade networks has the potential to give rise to a vast range of possible global food availability and scarcity scenarios in the current climate. A key challenge in preparing for this range of outcomes is that global warming is changing the probabilities of compound climate hazards in key agricultural regions (Sarhadi *et al* 2018). Given this non-stationarity, robustly quantifying the range of co-occurring climate hazards that could arise in the present climate is critical for ensuring anticipatory capacity for national governments, international trade policy, and agricultural-sector resilience.

In this work, we systematically quantify how regionally-extreme hot-and-dry or hot-and-wet conditions (Haqiqi *et al* 2021) are transmitted via international agricultural trade. Using the Global Trade Analysis Project (GTAP) economic trade database (Aguiar *et al* 2022), we focus on the four major staple crops that together account for the majority of calories consumed globally: wheat, maize, rice, and soya. A large single-model ensemble of gridded climate simulations (100 simulations of the Community Earth System Model 2, CESM2; (Simpson *et al* 2023, Danabasoglu *et al* 2020)) enables us to quantify the monthly occurrence of compound climate hazards across 100 different equally-likely realizations of the present-day climate (see Methods). Combining these climate simulations with agricultural production information (i.e. cropped area and growing season) along with the GTAP trade data reveals 100 internally-consistent realizations of how exposure to compound climate hazards may propagate via international agricultural trade in the near future.

Data and Methods

GTAP Trade Data

The GTAP database represents a consistent set of data on value flows within the global economy for a given reference year. It includes key input-output transactions in each region, bilateral international trade flows, capital stock and savings information, international transport costs, domestic input and output subsidies, export subsidies and import tariffs, and revenue flows from taxes and tariffs. In this study, we use version 11.b of the database for reference year 2017 which covers 160 regions and 65 commodities (Aguiar *et al* 2022). Paddy rice and wheat

sectors are explicitly defined in the database but maize and soya are aggregated together with similar crops and are included in cereal grain and oilseed sectors, respectively. We construct bilateral trade flows for these crop sectors using data on domestic sales (self-trade) as well as bilateral imports.

Calculation of compound climate hazards and exposure

Gridded, monthly near surface air temperature (variable name TREFHT) and precipitation (variable name PR) fields were obtained from the Community Earth System Model v2 Large Ensemble (CESM2-LE) (Simpson *et al* 2023, Danabasoglu *et al* 2020) which includes data from 1850-2100 under the historical and Shared Socio-economic Pathway 3-7.0 (Meinshausen *et al* 2020). The CESM2-LE consists of 100 realizations with the same forcing, but each realization is started from equally likely, but different, initial conditions (see Simpson et al. 2023 for details). Here, we focus only on the years 2015-2025 to estimate the range of climate outcomes arising from internal climate variability in the context of the current climate forcing.

Temperature and precipitation extremes are defined according to month-specific percentile thresholds defined over the 10-year baseline period of 2015-2024 across all 100 members. Thus, our baseline period spans 1000 simulated years (i.e., 10 years/realization x 100 realizations). Defining extremes based on percentiles, rather than fixed values, allows for the extremes to be specific to each gridpoint and implicitly removes any mean biases in the CESM2 Large Ensemble and MPI Grand Ensemble temperature and precipitation fields. Compound climate hazards in the 100 realizations of the year 2025 are defined as months when the temperature exceeds the month-specific 95th percentile over the baseline period and the precipitation either exceeds the 95th percentile over the baseline period (termed hot-and-wet) or is lower than the 5th percentile over the baseline period (termed hot-and-dry) (e.g., Haqiqi *et al* 2021).

For all analysis, we consider each of the four crops separately, only combining them at the calorie level after all other analysis is complete. For each crop, we analyze only grid points that are considered “cropped land” according to Tang et al. (2024), the most up-to-date geo-referenced global crop dataset of its kind. Then, for each of these grid points, we identify whether any of the months within the crop- and location-specific growing season are experiencing a compound climate hazard. Grid points experiencing hot-and-dry conditions that are also equipped with irrigation (Mehta *et al* 2024) are ignored. Specifically, the irrigation fields

are bilinearly re-gridded to the grid of the crop-level data of Tang et al. 2024, and all area equipped for irrigation within each gridcell is applied to every crop in that gridcell. Growing seasons containing both hot-and-wet and hot-and-dry conditions are treated as suffering from hot-and-wet hazards. We use Sachs et al. (2010) to define crop- and location-specific growing seasons, allowing for two growing seasons when specified.

For each crop, the above analysis leads to 100 gridded boolean maps of cropped gridpoints exposed to compound climate hazards. We then aggregate these results at the country level to obtain the fraction of cropped area within each country that is exposed for each of the 100 realizations. Specifically, we conservatively re-grid the crop-specific harvested area of Tang et al. (2024) to the grid of the CESM2 data to obtain the area fraction of each gridcell cropped. We then use these gridcell fractions to compute the fraction of the total cropped area exposed to compound climate hazards for each country for each realization. (Note that we also include an additional area-weighting due to the varying sizes of grid cells from the converging of longitudes at the poles.) The end result for each crop is thus a data set of shape 100 x 158, representing the fraction of cropped area exposed in 2025 across the 100 realizations and 158 countries.

From here, we combine these country-level metrics with the GTAP trade data to compute the fraction of total supply of each crop, to each country, exposed to compound climate hazards.

Conversion to Calories

To convert value flows for each crop to calories we construct global caloric conversion factors (in Kcal per USD). These conversion factors are calculated using global production for each crop (in metric tons) and crop-specific nutritive factors (calories per 100 grams) from FAOSTAT (FAO 2023) as well as Value of Production data in the GTAP database (Aguilar et al 2022). The crop-specific factors are 13.14 for wheat, 17.67 for maize, 5.66 for rice, and 8.08 for soya.

Phase Space Calculations

We also calculate the relationship between the number of major suppliers for each country versus the climate diversity among major suppliers. First, we quantify the number of major suppliers (x-axis) for each country as the number of suppliers required to reach 90% of the total caloric supply. Thus, countries with a single major supplier are those where 90% or more of the calories come from a single country. Self-trade is included in our calculations, so a country's top supplier is often itself. For countries with more than one major supplier, we sort their trade

partners by calorie contribution in descending order and define the number of major suppliers as the number of suppliers required for the cumulative contribution to exceed 90% of the country's total caloric imports.

Climate diversity is defined as the weighted-mean correlation of the percent of calories exposed to compound climate hazards of all major suppliers, with one another. For each country, for each of its major suppliers, we have a vector of 100 values signifying the percent of caloric supply exposed, one for each of the 100 realizations. We then correlate the vector for each major supplier with the vector of every other major supplier. This results in a set of correlations that signify how much each major supplier's exposure varies with that of the other major suppliers. Finally, we take a weighted-mean of these correlations, where the weights are computed as the fraction of calories contributed by the two suppliers to the reporter country. Higher weighted-mean correlations imply that the major suppliers' caloric supplies are exposed at similar times, while lower weighted-mean correlations imply that the major suppliers' caloric supplies are exposed more independently.

Clustering

We use the `sklearn.cluster.AgglomerativeClustering` module to cluster the country-level calories exposed to compound climate hazards (N = 158) across the 100 realizations (so our data has dimensions of 100x158). We perform agglomerative clustering using the "**`ward`**" linkage method which minimizes the variance (via a "**`euclidean`**" distance metric) of the clusters being merged. Agglomerative clustering is a hierarchical clustering method that starts at the individual sample level (in this case, our individual climate realizations) and recursively pairs samples, and then groups of samples, that look most like one another until all samples have been clustered together. For our discussion, we focus on seven clusters which are determined via a distance threshold to halt the merging of the clusters. We visualize each cluster by the median across all realizations within that cluster.

Results

For each country in the GTAP database, we calculate the percentage of its crop-specific supply that is exposed to compound climate hazards in each of the 100 realizations (Fig. 1; Supp. Text T1). Here we define compound climate hazards by months that are both in the hottest 5% of months and are also in either the wettest or driest 5% of months (see Methods), removing months experiencing hot-and-dry compound climate hazards for areas equipped for irrigation

(see Methods; (61)). Since many countries serve as their own predominant source of calories, we include self-trade in our analysis and refer to crop "supply" as the combination of domestic consumption and imports from other countries. We find that there is substantial potential for trade in calories exposed to compound climate hazards at current levels of global warming, based on 100 equally-likely realizations of the annual global climate (Fig. 2).

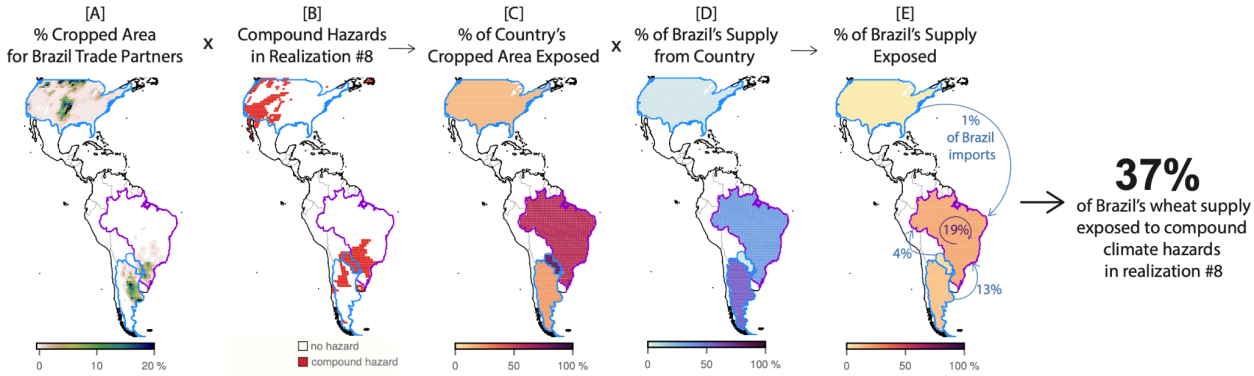

Figure 1. Example workflow combining growing-season specific compound climate hazards with cropped area and the GTAP trade data to quantify the percentage of Brazil's wheat supply exposed within a given climate model realization (in this example, realization #8).

Physically consistent realizations depict the fraction of food supply exposed to compound climate hazards (Fig. 2A,B). For example, for wheat, one worst-case realization depicts a world where 20% or more of wheat supply in nearly half of the countries in the world are exposed to compound climate hazards (member #99; Fig 2C). Hotspots in this realization include Eastern Europe, parts of the Middle East, and much of Africa. Contrast this with a best-case realization, where less than 1% of countries have greater than 20% of their wheat supply exposed (Fig 2D). We emphasize that because the differences in the distributions of exposure to compound climate hazards arise primarily from internal climate variability, these realizations represent equally plausible outcomes. Similar analyses for maize, rice, and soya are provided in the Supplement (Supp. Fig. 1-3) and demonstrate large differences between best- and worst-case realizations across all four crops (0%-24% of countries for maize, 1%-17% for rice, and 0%-20% for soya).

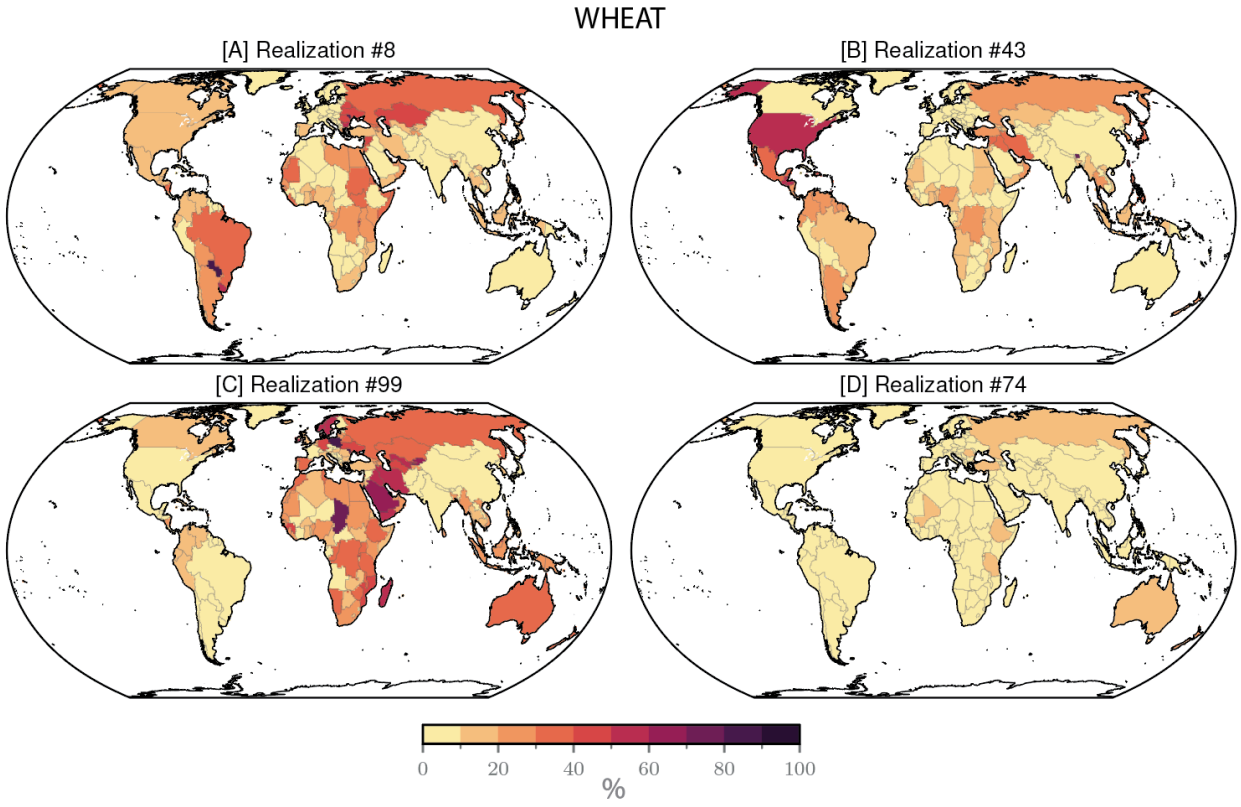

Figure 2. Fraction of wheat supplies exposed to compound climate hazards, arising from international trade with 0% corresponding to none of the wheat supply exposed, and 100% corresponding to all of the wheat supply exposed. (A,B) Offers two examples of diverse outcomes (realizations #8 and #43); (C) is a worst-case realization where 44% of countries have 20% or more of their wheat supply exposed (realization #99); (D) is a best-case realization where less than 1% of countries have 20% or more of their wheat supply exposed (realization #54).

Individual countries show substantial variation in their percentage of exposed wheat supply across the 100 climate realizations. Furthermore, countries differ greatly from each other in the range of exposure due to the unique combination of their wheat-specific trade network and the climates of their wheat suppliers. This is quantified by calculating the range of fractional wheat supply that is exposed to compound climate hazards across the 100-member ensemble (i.e., the maximum and minimum percentages of exposed wheat supply) for a subset of countries (Fig. 3). The bottom-heavy distributions in Figure 3 demonstrate that, in general, most realizations are characterized by low percentages of exposed supply since compound climate hazards are, by our definition, relatively rare. However, there is heterogeneity in the severity of the worst-case realizations (i.e. the maximum percentage of exposed supply for each country; see also Supp. Fig. 6B) across the 100 realizations. For example, Serbia has a worst-case realization where 99% of its wheat supply is exposed to compound climate hazards. This

worst-case realization is not a single outlier either, as at least 11 other realizations show the majority of Serbia's wheat supply exposed. Comparatively, Nigeria has a much less severe worst-case realization of <30% of its wheat supply exposed. Moreover, the majority of its climate realizations experience <10% of its supply exposed.

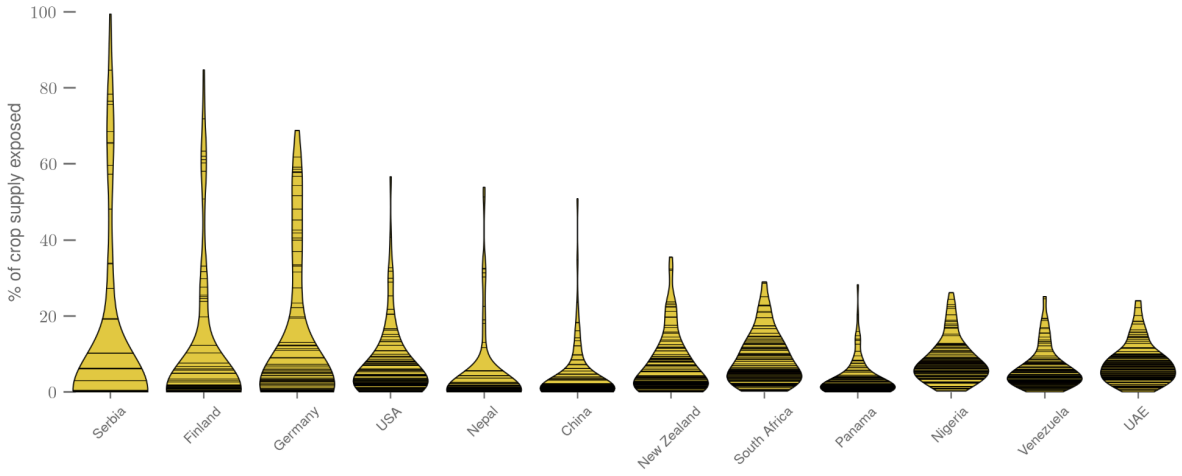

Figure 3. Percentage of total wheat supply exposed to compound climate hazards for a sample of 14 countries across the 100 realizations. The length of the yellow 'violins' correspond to the country-level range of the fraction of supply exposed, the horizontal black lines denote individual realizations, and the width of the violins correspond to the density of realizations within a particular range.

We generalize our analysis by converting the four crops (wheat, maize, rice, and soya) into their corresponding caloric content (Supp. Fig. 4, Supp. Fig. 15). This conversion allows for investigations into overall caloric availability across the crops, and the food security implications of compound climate hazard exposure transmitted through trade. Ensemble member #99 is also a worst-case realization for calories, as it was for wheat alone, although the map of exposed caloric supplies across countries highlights mid-to-southern Africa as particularly negatively impacted due to their heavy reliance on maize production and consumption (Supp. Fig. 4C; Supp. Fig. 15). While the GTAP database labels all countries as their own top supplier of calories (not shown), the average importance of imports for exposed caloric supply varies significantly from country-to-country (Fig. 4A). Much of Africa, the Middle East, and Europe exhibit, on average, >50% of their exposed caloric supply as coming from their trade partners, while for large countries like India and the USA that span more agro-ecological zones obtain almost all of their exposed caloric supply from themselves (Fig. 4A).

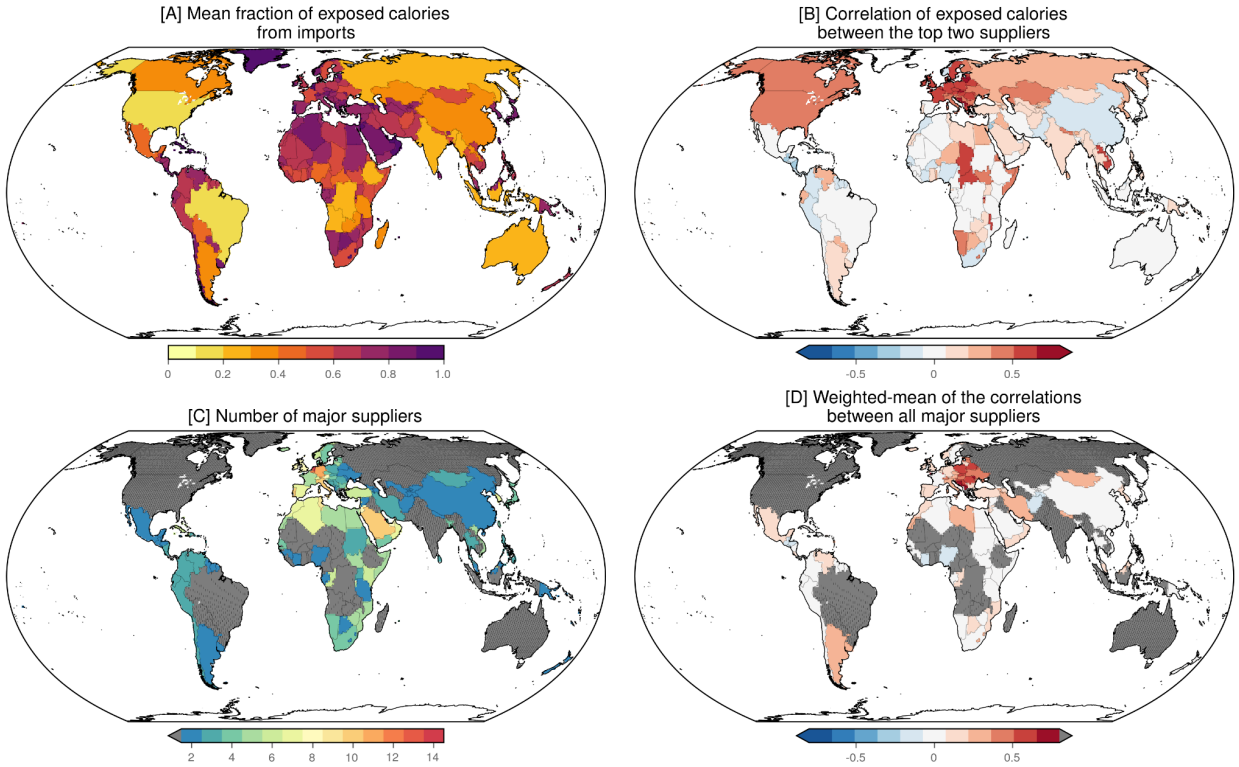

Figure 4. Supplies of calories exposed to compound climate hazards, summarized across all 100 climate realizations; (A) mean fraction of exposed calories that come from imports; (B) correlation of exposed calories between the top two suppliers for each country; (C) number of major suppliers of calories for each country (see Methods) and (D) the weighted-mean of the correlations between all pairs of major suppliers across the 100 climate realizations. Gray shading denotes countries that are their own, single, major supplier in panel C and thus have a correlation of exactly 1.0 in panel D.

High percentages of exposed caloric supply can arise if the major suppliers to a given country experience compound climate hazards simultaneously. To quantify this, we compute the correlation across the 100 realizations of the exposed caloric supply between the top two suppliers (based on calories) for each country (Fig. 4B). Note that one of the top two suppliers may be the country itself (Fig. 4C). The northern hemisphere temperate countries tend to have the highest correlations, indicating that when the top supplier's crops are exposed to compound climate hazards, those of the second top supplier are as well. European countries exhibit some of the highest correlations globally. These high, positive correlations are due, in part, to the fact that European countries have many policies to facilitate significant intra-European trade (Aguiar *et al* 2022) and that Europe often experiences compound climate hazards across many countries simultaneously (Markonis *et al* 2021). Negative correlations are equally of interest (e.g. Nigeria) as they denote countries who's top two suppliers act as buffers to one another: if one supplier's crops are exposed, those of the other likely are not.

We further extend this analysis to include a summary of the correlations across *all* major suppliers (defined as the number of suppliers necessary to provide 90% of the country's total caloric supply). Figure 4D depicts the weighted-mean of all correlations of exposed caloric supplies among major suppliers for a country. With this definition, a significant number of countries are their own, sole, major supplier, giving rise to correlations of 1.0. Many European countries have four or more major suppliers (see also Fig. 4C), which increases the climate-diversity across suppliers and reduces the correlations in Figure 4D.

Countries with fewer major suppliers (in terms of calories) may be particularly vulnerable to compound climate hazards if those suppliers share similar temporal evolutions in their weather and climate patterns (Fig. 4D). Thus, we explore whether countries with low levels of diversification, in terms of both the number and climates of their suppliers, are more likely to experience large fractions of exposed caloric supply. We use each country's "worst case" realization across all 100 to illustrate this relationship between climate and trade partner diversification in a two-dimensional phase space (Fig. 5; see Methods). We draw specific attention to four regions of the phase space. First, countries with only one major supplier will, by definition, appear in the upper-left-hand corner (dashed box). These countries, such as Finland, Brazil and Niger (Fig. 4C) have the lowest import and climate diversification possible, and the majority of these countries have worst-case realizations where more than 70% of their total imported calories are exposed to compound climate hazards (Fig. 5 inset; Supp. Fig. 6A). Those that do not experience these extreme worst-case realizations tend to be geographically large countries (e.g. USA, Australia, Russia); this spatial scale likely provides for climate diversity across the country itself (though this protection is not universal for geographically large countries, as in the case of Brazil; Supp. Fig. 6A).

Second, some countries have only a few suppliers (3 or fewer) that are highly correlated in their climate variability (Fig. 4D; Fig. 5), implying that the regions are not independent from one another in terms of compound climate hazards. Croatia and Slovenia are examples of two countries with both low diversification in trading partners and high correlation of their partners' climate variability. For example, Croatia and its other major supplier, Hungary, border one another and are thus more likely to experience compound climate hazards at the same time. Figure 5 shows that countries like Croatia with low diversification in terms of both number of suppliers (x-axis) and supplier climates (y-axis) tend to experience more severe worst-case realizations (i.e., a larger percentage of exposed caloric supply; Supp. Fig. 6A).

Third, countries with only a few suppliers that have largely independent climates (i.e. small or negative correlations) tend to fare better in terms of their worst-case realizations. The

Dominican Republic serves as a good example of this, where its three major suppliers are not correlated with one another, and its worst-case realization across all 100 realizations is 22% of its caloric supply exposed to compound climate hazards (Supp. Fig. 6A).

Fourth, all countries with six or more major suppliers (e.g. the United Arab Emirates) experience low correlations across suppliers and tend to have less severe worst-case realizations. In general, Figure 5 suggests that poor diversification in terms of supplier climates (larger y-axis values) is associated with more severe worst-case possibilities across the 100 realizations.

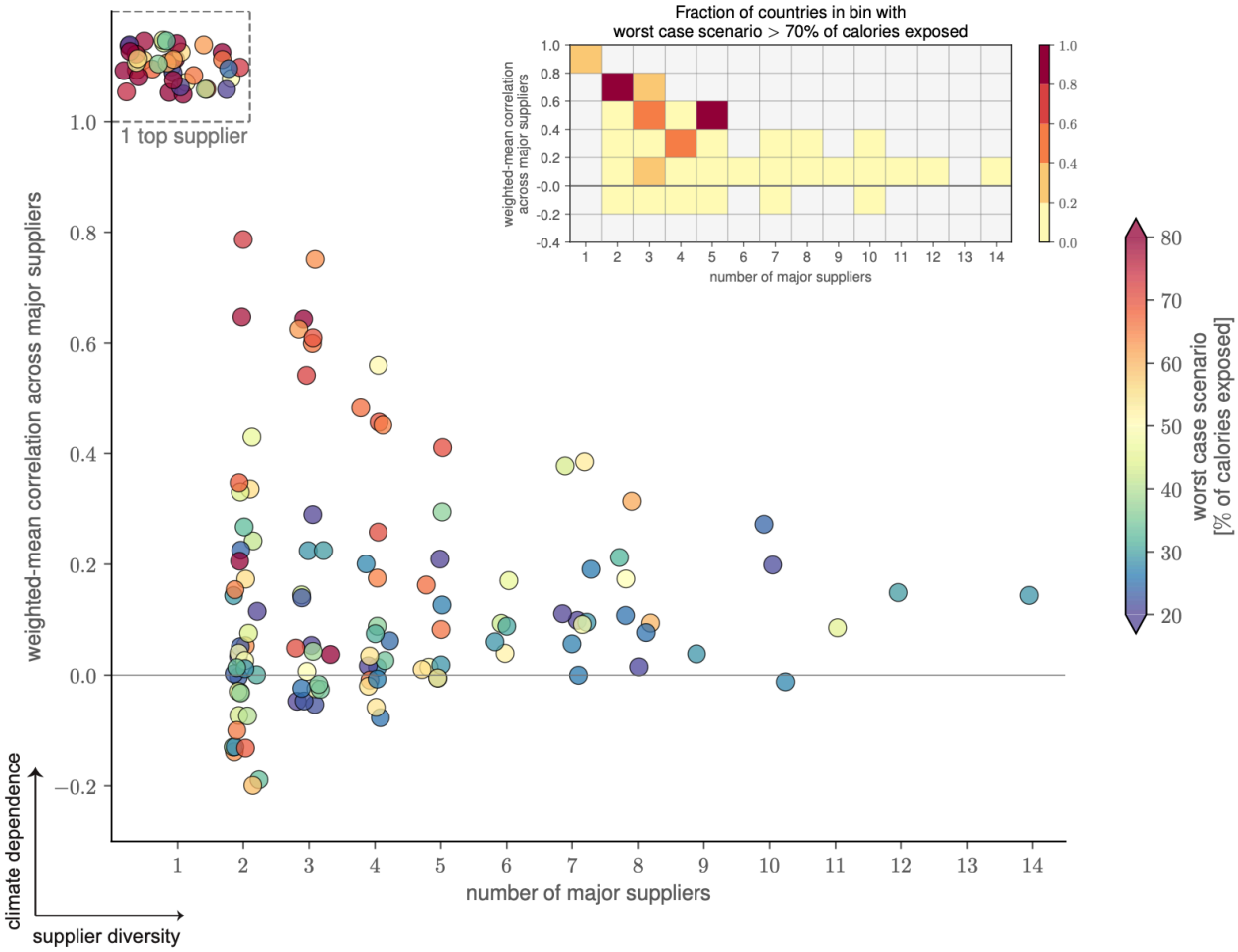

Figure 5. Calorie supply diversification phase space showing supplier diversification on the x-axis (i.e., number of major suppliers) versus the climate diversification across suppliers on the y-axis (i.e. average correlation across pairs of major suppliers). Countries in the upper-left-hand corner (dashed box), are their own, sole major supplier. To improve the visualization of countries with the same x-axis value, each dot is randomly shifted slightly to the right or left along the x-axis.

The phase diagram reveals relationships arising from diversity in the number of suppliers and diversity in supplier climates *across* the 100 realizations. While this can provide insights into

the underlying climate and trade dynamics of the system, in reality only one realization of the climate system can exist at any one time. To quantify and summarize the prevalence of particular realizations we cluster the 100 climate realizations based on the fraction of caloric supply exposed to compound climate hazards across all countries, producing seven 'archetypal' clusters that are constrained by the dynamics of the physical climate system (Fig. 6; Supp. Fig. 7). The goal here is to provide insight into key geospatial patterns of exposed caloric supplies, in service of anticipatory policy that can help reduce food insecurity and economic disruption.

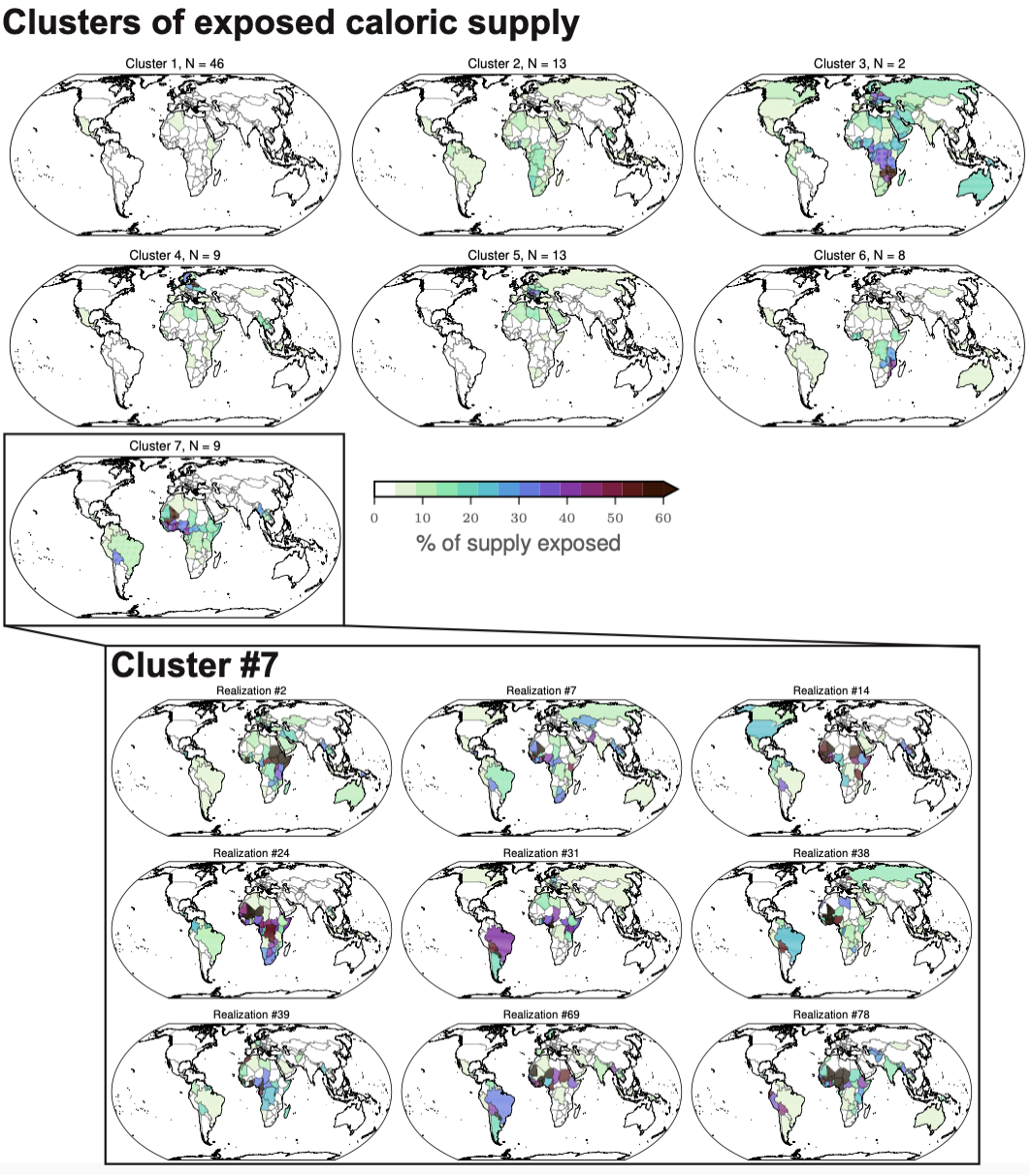

Figure 6. Seven clusters of the 100 realizations, summarized as maps of the median realization of caloric supply exposed to compound climate hazards across realizations within each cluster. Inset shows the seven specific realizations that comprise Cluster #7 wherein West Africa is particularly exposed.

The median 'archetypal' realization of each of the seven clusters are depicted in Figure 6. The archetype encompassing the most climate realizations (Cluster #1; N=46) shows a world characterized by very low fractions of exposed caloric supply, globally. Cluster #3, on the other hand, summarizes realizations where eastern Europe and southern Africa exhibit high fractions of exposed caloric supply, although this cluster only comprises two of the 100 realizations. This may be, in part, because Cluster #5 captures additional realizations where eastern Europe's caloric supply sees substantial exposure to compound climate hazards. Cluster #7 is further expanded in the inset to show its nine realizations. While no single realization is identical to another, the consistent pattern across all of the realizations is substantial exposure across countries in West Africa and South America. These realizations are of particular interest as West Africa is experiencing very high population growth with growing dependence on imports (35). Thus, Cluster #7 summarizes a set of realizations that would greatly increase the risk of food insecurity in the region. Nigeria serves as an interesting counterpoint to this. With its two major suppliers of calories (itself and the United States) negatively correlated in their climates (r=-0.12; Fig. 4D), its worst-case realization for calories is lower than that of many of its West African neighbors (Supp. Fig. 14).

Discussion

Our results highlight the patterns of compound climate hazard exposure that may be transmitted globally through the flow of international agricultural trade. We find that diversification of suppliers' climate generally corresponds to overall lower exposure of its caloric supply to climate hazards. Broadly speaking, increasing trade partner diversity (especially supplier diversity) is a well-understood strategy to reduce exposure to specific trade partner hazards (Hertel *et al* 2021). At the same time, international food trade is a key mechanism for risk propagation internationally (Centeno *et al* 2015). Thus, while increasing trade partner diversity reduces exposure to climate hazards arising in specific trade partners, the broad trend of increased reliance on imported food increases overall exposure to distant climate hazards. Further, evidence suggests that spatial correlation in staple commodity production in the presence of increasing trade has contributed to increased inequality, with the benefits accruing disproportionately to the high productivity regions (Dingel *et al* 2019).

Our results contribute to the growing body of work on the subject of what has been termed 'complex' or 'systemic' climate risk (Centeno *et al* 2015, Simpson *et al* 2021, Westra and Zscheischler 2023) in the context of the globalized food system (Mehrabi *et al* 2022, Gaupp *et al* 2019), specifically, how countries may become exposed to suppliers' climate hazards via

international trade (Hedlund *et al* 2018, 2022). Others have considered the quantifiable relationships between compound climate extremes and agricultural productivity operating both through the impacts on plants, as well as through the impact on agricultural workers (Biess *et al* 2024, Haqiqi *et al* 2021, De Lima *et al* 2021, Lesk *et al* 2022). Jägermeyr et al. (2021) quantify the likely impacts of climate change on staple crop yields and find that the uncertainty associated with some crop models is far greater than the uncertainty owing to climate models alone. Furthermore, some of these simulation results are at odds with meta-analyses of crop yield impacts from a changing climate (Moore *et al* 2017). Additionally, climate extremes affect crop production and caloric availability through multiple channels, not just plant stress. Recent studies show that the impact on agricultural labor of moist heat can rival and even surpass the impacts of climate extremes on crop production (De Lima *et al* 2021). Comprehensive analyses of all the potential pathways through which compound extremes affect staple crops remains an avenue for future research, which will require a stronger consensus about the physiological channels of impact, as well as a much more substantial computational undertaking than what is feasible in this study alone. The work reported here aims to quantitatively motivate such future studies, highlighting the importance of sampling a wide range of internal climate variability moving forward.

Notably, our analysis reveals pockets of resilience in global agricultural trade, in the form of negative correlations in exposed caloric supplies (e.g., blue areas in Fig. 4B,D). Diverse trading partners correspond to lower magnitudes of exposed caloric supplies (Kummu *et al* 2020), and may thus serve to buffer against local threats to supplies. An extension of this finding could aim to reveal how sources of resilience may ebb and flow, as the economy dynamically responds to exposure to compound climate hazards. For example, beyond imports, export restrictions by countries seeking to mitigate the impact of globally threatened commodity markets on domestic consumers may further accelerate climate risk (Anderson and Nelgen 2012, Ahmed *et al* 2012). Future work could also explore scenarios of trade dynamics to inform strategic configuration of suppliers to provide optimal climate diversification.

Further, an adaptation strategy using diversification to distribute risk and improve resilience may inadvertently assume that global crop production will, or can be, largely maintained into the future. If a particularly climate-sensitive crop were to become exposed in most or all of its productive geography under future climate change conditions, overall global supply would be affected regardless of diversification. Thus, trade diversification of partners may be less suitable for climate-change-sensitive crops. In such cases, resilience may come from diversifying to other crops rather than partners (Jägermeyr *et al* 2021).

Our emphasis in this analysis is on robustly quantifying the potential for exposure to compound climate hazards in the current climate. Yet, the archetypal climate realizations (Fig. 6) may also help to characterize potential future worlds affected by climate hazards. This information could be fruitfully combined with seasonal-to-decadal predictions of climate, opening a window into the types of international trade conditions that could unfold in the near term (Dunstone *et al* 2022). Specifically, combining initialized seasonal-to-decadal predictions of the climate with a dynamic economic model of agricultural trade could permit the creation of testable hypotheses about future compound climate hazards and how they propagate around the planet.

This leads more generally into future work to combine the present analysis with robust models of international trade and the global economy. How are patterns of international trade likely to evolve in the context of climate-related disruptions (Baldos *et al* 2019)? Is it possible to anticipate these disruptions (Nóia Júnior *et al* 2022)? We recommend future work incorporating more detailed trade analysis to characterize economic dynamics that might modulate trade in exposed goods, including the substitutability across suppliers and among different food commodities. Detailed economic trade analysis would permit a deeper investigation, and would allow analysis to go beyond crop and caloric supplies to account for the impact on the broader economy and human welfare (Baldos *et al* 2019).

A further consideration of this work is the use of a single model ensemble. Each climate model has its own biases, both for large-scale modes of climate variability and regional climate dynamics (Giorgi and Coppola 2010). Thus, a different single-model ensemble could result in different spatial distributions of exposed caloric supplies, globally. With that said, we repeated our analysis for the 100 members of the MPI Grand Ensemble (Maher *et al* 2019) under the CMIP5 RCP4.5 scenario (Meinshausen *et al* 2011) and found very similar results (see Supp. Fig. 8-13). Nonetheless, this motivates continued investment in large ensembles from multiple climate models.

Conclusion

We seek to robustly quantify the range of co-occurring climate hazards that could arise primarily from internal variability in the present climate, and how that exposure is transmitted through global agricultural trade networks to shape the exposure of individual countries. We deliberately focus on present-day exposure rather than future exposure to anthropogenic climate change to understand the full range of outcomes that are physically possible in the context of existing practices, climate, and trade networks. We find that in general the fraction of a country's caloric

supply exposed to compound climate hazards increases as the diversity of its suppliers decreases. Notably, this is true not only for the number of trading partners but also for diversity among supplier climates, as physical connections in the global climate system regulate the co-occurence of compound hazards between different regions. This work contributes to the growing literature on the threat posed by tele-connected climate hazards and international agricultural trade. While the risks posed by continued global warming have been frequently documented, we demonstrate that internal climate variability has the potential to substantially aggravate the exposure of global trade networks in climate-sensitive sectors, with potential implications for global, regional and local food security.

References

AghaKouchak A, Chiang F, Huning L S, Love C A, Mallakpour I, Mazdiyasni O, Moftakhari H, Papalexiou S M, Ragno E and Sadegh M 2020 Climate Extremes and Compound Hazards in a Warming World *Annu. Rev. Earth Planet. Sci.* **48** 519–48

Aguiar A, Chepeliev M, Corong E and van der Mensbrugghe D 2022 The Global Trade Analysis Project (GTAP) Data Base: Version 11 *JGEA* **7** Online: https://www.jgea.org/ojs/index.php/jgea/article/view/181

Ahmed S A, Diffenbaugh N S, Hertel T W and Martin W J 2012 Agriculture and trade opportunities for Tanzania: Past volatility and future climate change *Rev. Dev. Econ.* **16** 429–47

Anderson K and Nelgen S 2012 Agricultural trade distortions during the global financial crisis *Oxford Review of Economic Policy* **28** 235–60

Anderson W, Baethgen W, Capitanio F, Ciais P, Cook B I, Cunha C G R da, Goddard L, Schauberger B, Sonder K, Podestá G, van der Velde M and You L 2023 Climate variability and simultaneous breadbasket yield shocks as observed in long-term yield records *Agric. For. Meteorol.* **331** 109321

Baldos U L C and Hertel T W 2015 The role of international trade in managing food security risks from climate change *Food Security* **7** 275–90

Baldos U L C, Hertel T W and Moore F C 2019 Understanding the spatial distribution of welfare impacts of global warming on agriculture and its drivers *Am. J. Agric. Econ.* **101** 1455–72

Bevacqua E, Suarez-Gutierrez L, Jézéquel A, Lehner F, Vrac M, Yiou P and Zscheischler J 2023 Advancing research on compound weather and climate events via large ensemble model simulations *Nat. Commun.* **14** 2145

Biess B, Gudmundsson L, Windisch M G and Seneviratne S I 2024 Future changes in spatially compounding hot, wet or dry events and their implications for the world's breadbasket regions *Environ. Res. Lett.* **19** 064011

Carter T R, Benzie M, Campiglio E, Carlsen H, Fronzek S, Hildén M, Reyer C P O and West C 2021 A conceptual framework for cross-border impacts of climate change *Glob. Environ. Change* **69** 102307

Centeno M A, Nag M, Patterson T S, Shaver A and Windawi A J 2015 The Emergence of Global Systemic Risk *Annu. Rev. Sociol.* **41** 65–85

Challinor A J, Adger W N and Benton T G 2017 Climate risks across borders and scales *Nat. Clim. Chang.* **7** 621–3

Dalin C, Konar M, Hanasaki N, Rinaldo A and Rodriguez-Iturbe I 2012 Evolution of the global virtual water trade network *Proc. Natl. Acad. Sci. U. S. A.* **109** 5989–94

Danabasoglu G, Lamarque J-F, Bacmeister J, Bailey D A, DuVivier A K, Edwards J, Emmons L K, Fasullo J, Garcia R, Gettelman A, Hannay C, Holland M M, Large W G, Lauritzen P H, Lawrence D M, Lenaerts J T M, Lindsay K, Lipscomb W H, Mills M J, Neale R, Oleson K W,

Otto-Bliesner B, Phillips A S, Sacks W, Tilmes S, Kampenhout L, Vertenstein M, Bertini A, Dennis J, Deser C, Fischer C, Fox-Kemper B, Kay J E, Kinnison D, Kushner P J, Larson V E, Long M C, Mickelson S, Moore J K, Nienhouse E, Polvani L, Rasch P J and Strand W G 2020 The community earth system model version 2 (CESM2) *J. Adv. Model. Earth Syst.* **12** Online: https://agupubs.onlinelibrary.wiley.com/doi/10.1029/2019MS001916

De Lima C Z, Buzan J R, Moore F C, Baldos U L C, Huber M and Hertel T W 2021 Heat stress on agricultural workers exacerbates crop impacts of climate change *Environ. Res. Lett.* **16** 044020

Diaz C D, Ting M, Horton R, Singh D, Rogers C D W and Coffel E 2023 Increased extreme humid heat hazard faced by agricultural workers *Environ. Res. Commun.* **5** 115013

Dingel J I, Meng K C and Hsiang S M 2019 Spatial Correlation, Trade, and Inequality: Evidence from the Global Climate Online: http://www.nber.org/papers/w25447

Dunstone N, Lockwood J, Solaraju-Murali B, Reinhardt K, Tsartsali E E, Athanasiadis P J, Bellucci A, Brookshaw A, Caron L-P, Doblas-Reyes F J, Früh B, González-Reviriego N, Gualdi S, Hermanson L, Materia S, Nicodemou A, Nicolì D, Pankatz K, Paxian A, Scaife A, Smith D and Thornton H E 2022 Towards Useful Decadal Climate Services *Bull. Am. Meteorol. Soc.* **103** E1705–19

Ebi K L, Capon A, Berry P, Broderick C, de Dear R, Havenith G, Honda Y, Kovats R S, Ma W, Malik A, Morris N B, Nybo L, Seneviratne S I, Vanos J and Jay O 2021 Hot weather and heat extremes: health risks *Lancet* **398** 698–708

Ercin E, Veldkamp T I E and Hunink J 2021 Cross-border climate vulnerabilities of the European Union to drought *Nat. Commun.* **12** 3322

FAO 2023 *World Food and Agriculture – Statistical Yearbook 2023* (Rome: Food & Agriculture Organization) Online: http://dx.doi.org/10.4060/cc8166en

Field C B, Barros V, Stocker T F and Dahe Q 2012 *Managing the Risks of Extreme Events and Disasters to Advance Climate Change Adaptation: Special Report of the Intergovernmental Panel on Climate Change* (Cambridge University Press)

Gaupp F, Hall J, Hochrainer-Stigler S and Dadson S 2019 Changing risks of simultaneous global breadbasket failure *Nat. Clim. Chang.* **10** 54–7

Giorgi F and Coppola E 2010 Does the model regional bias affect the projected regional climate change? An analysis of global model projections *Clim. Change* **100** 787–95

Haqiqi I, Grogan D S, Hertel T W and Schlenker W 2021 Quantifying the impacts of compound extremes on agriculture *Hydrol. Earth Syst. Sci.* **25** 551–64

Hedlund J, Carlsen H, Croft S, West C, Bodin Ö, Stokeld E, Jägermeyr J and Müller C 2022 Impacts of climate change on global food trade networks *Environ. Res. Lett.* **17** 124040

Hedlund J, Fick S, Carlsen H and Benzie M 2018 Quantifying transnational climate impact exposure: New perspectives on the global distribution of climate risk *Glob. Environ. Change* **52** 75–85

Heino M, Kinnunen P, Anderson W, Ray D K, Puma M J, Varis O, Siebert S and Kummu M 2023

Increased probability of hot and dry weather extremes during the growing season threatens global crop yields *Sci. Rep.* **13** 3583

Hertel T, Elouafi I, Tanticharoen M and Ewert F 2021 Diversification for enhanced food systems resilience *Nat Food* **2** 832–4

Hertel T W and de Lima C Z 2020 Viewpoint: Climate impacts on agriculture: Searching for keys under the streetlight *Food Policy* **95** 101954

Hoeppe P 2016 Trends in weather related disasters – Consequences for insurers and society *Weather Clim. Extrem.* **11** 70–9

Jägermeyr J, Müller C, Ruane A C, Elliott J, Balkovic J, Castillo O, Faye B, Foster I, Folberth C, Franke J A, Fuchs K, Guarin J R, Heinke J, Hoogenboom G, Iizumi T, Jain A K, Kelly D, Khabarov N, Lange S, Lin T-S, Liu W, Mialyk O, Minoli S, Moyer E J, Okada M, Phillips M, Porter C, Rabin S S, Scheer C, Schneider J M, Schyns J F, Skalsky R, Smerald A, Stella T, Stephens H, Webber H, Zabel F and Rosenzweig C 2021 Climate impacts on global agriculture emerge earlier in new generation of climate and crop models *Nature Food* **2** 873–85

Kummu M, Kinnunen P, Lehikoinen E, Porkka M, Queiroz C, Röös E, Troell M and Weil C 2020 Interplay of trade and food system resilience: Gains on supply diversity over time at the cost of trade independency *Global Food Security* **24** 100360

Lee M-S, Kang B-M, Lee J-E, Choi W-J, Ko J, Choi J-E, An K-N, Kwon O-D, Park H-G, Shin H-R, Lee I, Kim J-K and Kim H-Y 2013 How do extreme wet events affect rice quality in a changing climate? *Agric. Ecosyst. Environ.* **171** 47–54

Lesk C, Anderson W, Rigden A, Coast O, Jägermeyr J, McDermid S, Davis K F and Konar M 2022 Compound heat and moisture extreme impacts on global crop yields under climate change *Nature Reviews Earth & Environment* **3** 872–89

Li Y, Guan K, Schnitkey G D, DeLucia E and Peng B 2019 Excessive rainfall leads to maize yield loss of a comparable magnitude to extreme drought in the United States *Glob. Chang. Biol.* **25** 2325–37

Maher N, Milinski S, Suarez-Gutierrez L, Botzet M, Dobrynin M, Kornblueh L, Kröger J, Takano Y, Ghosh R, Hedemann C, Li C, Li H, Manzini E, Notz D, Putrasahan D, Boysen L, Claussen M, Ilyina T, Olonscheck D, Raddatz T, Stevens B and Marotzke J 2019 The Max Planck Institute Grand Ensemble: enabling the exploration of climate system variability *J. Adv. Model. Earth Syst.* **11** 2050–69

Markonis Y, Kumar R, Hanel M, Rakovec O, Máca P and AghaKouchak A 2021 The rise of compound warm-season droughts in Europe *Sci Adv* **7** Online: http://dx.doi.org/10.1126/sciadv.abb9668

Mehrabi Z, Delzeit R, Ignaciuk A, Levers C, Braich G, Bajaj K, Amo-Aidoo A, Anderson W, Balgah R A, Benton T G, Chari M M, Ellis E C, Gahi N Z, Gaupp F, Garibaldi L A, Gerber J S, Godde C M, Grass I, Heimann T, Hirons M, Hoogenboom G, Jain M, James D, Makowski D, Masamha B, Meng S, Monprapussorn S, Müller D, Nelson A, Newlands N K, Noack F, Oronje M, Raymond C, Reichstein M, Rieseberg L H, Rodriguez-Llanes J M, Rosenstock T, Rowhani P, Sarhadi A, Seppelt R, Sidhu B S, Snapp S, Soma T, Sparks A H, Teh L,

Tigchelaar M, Vogel M M, West P C, Wittman H and You L 2022 Research priorities for global food security under extreme events *One Earth* **5** 756–66

Mehta P, Siebert S, Kummu M, Deng Q, Ali T, Marston L, Xie W and Davis K F 2024 Half of twenty-first century global irrigation expansion has been in water-stressed regions *Nature Water* **2** 254–61

Meinshausen M, Nicholls Z R J, Lewis J, Gidden M J, Vogel E, Freund M, Beyerle U, Gessner C, Nauels A, Bauer N, Canadell J G, Daniel J S, John A, Krummel P B, Luderer G, Meinshausen N, Montzka S A, Rayner P J, Reimann S, Smith S J, van den Berg M, Velders G J M, Vollmer M K and Wang R H J 2020 The shared socio-economic pathway (SSP) greenhouse gas concentrations and their extensions to 2500 *Geosci. Model Dev.* **13** 3571–605

Meinshausen M, Smith S J, Calvin K, Daniel J S, Kainuma M L T, Lamarque J-F, Matsumoto K, Montzka S A, Raper S C B, Riahi K, Thomson A, Velders G J M and van Vuuren D P P 2011 The RCP greenhouse gas concentrations and their extensions from 1765 to 2300 *Clim. Change* **109** 213

Merz B, Blöschl G, Vorogushyn S, Dottori F, Aerts J C J H, Bates P, Bertola M, Kemter M, Kreibich H, Lall U and Macdonald E 2021 Causes, impacts and patterns of disastrous river floods *Nature Reviews Earth & Environment* **2** 592–609

Mondal S, K Mishra A, Leung R and Cook B 2023 Global droughts connected by linkages between drought hubs *Nat. Commun.* **14** 144

Moore F C, Baldos U, Hertel T and Diaz D 2017 New science of climate change impacts on agriculture implies higher social cost of carbon *Nat. Commun.* **8** 1607

Nóia Júnior R de S, Ewert F, Webber H, Martre P, Hertel T W, van Ittersum M K and Asseng S 2022 Needed global wheat stock and crop management in response to the war in Ukraine *Global Food Security* **35** 100662

Parent C, Capelli N, Berger A, Crèvecoeur M and Dat J 2008 An overview of plant responses to soil waterlogging *Plant stress* **2** 20–7

Ridder N N, Ukkola A M, Pitman A J and Perkins-Kirkpatrick S E 2022 Increased occurrence of high impact compound events under climate change *npj Climate and Atmospheric Science* **5** 1–8

Sachs J, Remans R, Smukler S, Winowiecki L, Andelman S J, Cassman K G, Castle D, DeFries R, Denning G, Fanzo J, Jackson L E, Leemans R, Lehmann J, Milder J C, Naeem S, Nziguheba G, Palm C A, Pingali P L, Reganold J P, Richter D D, Scherr S J, Sircely J, Sullivan C, Tomich T P and Sanchez P A 2010 Monitoring the world's agriculture *Nature Publishing Group UK* Online: http://dx.doi.org/10.1038/466558a

Sarhadi A, Ausín M C, Wiper M P, Touma D and Diffenbaugh N S 2018 Multidimensional risk in a nonstationary climate: Joint probability of increasingly severe warm and dry conditions *Sci Adv* **4** eaau3487

Schlenker W and Roberts M J 2009 Nonlinear temperature effects indicate severe damages to U.S. crop yields under climate change *Proceedings of the National Academy of Sciences*

106 15594–8

Simpson I R, Rosenbloom N, Danabasoglu G, Deser C, Yeager S G, McCluskey C S, Yamaguchi R, Lamarque J-F, Tilmes S, Mills M J and Rodgers K B 2023 The CESM2 Single-Forcing Large Ensemble and Comparison to CESM1: Implications for Experimental Design *J. Clim.* **36** 5687–711

Simpson N P, Mach K J, Constable A, Hess J, Hogarth R, Howden M, Lawrence J, Lempert R J, Muccione V, Mackey B, New, Mark G., O'Neill B, Otto F, Pörtner H-O, Reisinger A, Roberts D, Schmidt D N, Seneviratne S, Strongin S, van Aalst M, Totin E and Trisos C H 2021 A framework for complex climate change risk assessment *One Earth* **4** 489–501

Singh D, Crimmins A R, Pflug J M, Barnard P L, Helgeson J F, Hoell A, Jacobs F H, Jacox M G, Jerolleman A and Wehner M F 2023 Focus on compound events *Fifth National Climate Assessment* ed A R Crimmins, C W Avery, D R Easterling, K E Kunkel, B C Stewart and T K Maycock (Washinton, D.C., USA: U.S. Global Change Research Program)

Singh J, Ashfaq M, Skinner C B, Anderson W B, Mishra V and Singh D 2022 Enhanced risk of concurrent regional droughts with increased ENSO variability and warming *Nat. Clim. Chang.* **12** 163–70

Tang F H M, Nguyen T H, Conchedda G, Casse L, Tubiello F N and Maggi F 2024 CROPGRIDS: a global geo-referenced dataset of 173 crops *Sci Data* **11** 413

Urban D W, Roberts M J, Schlenker W and Lobell D B 2015 The effects of extremely wet planting conditions on maize and soybean yields *Clim. Change* **130** 247–60

Vecellio D J, Kong Q, Kenney W L and Huber M 2023 Greatly enhanced risk to humans as a consequence of empirically determined lower moist heat stress tolerance *Proc. Natl. Acad. Sci. U. S. A.* **120** e2305427120

Verma M, Hertel T and Diffenbaugh N 2014 Market-oriented ethanol and corn-trade policies can reduce climate-induced US corn price volatility *Environ. Res. Lett.* **9** 064028

Westra S and Zscheischler J 2023 Accounting for systemic complexity in the assessment of climate risk *One Earth* **6** 645–55

Zscheischler J and Seneviratne S I 2017 Dependence of drivers affects risks associated with compound events *Sci Adv* **3** e1700263

Zscheischler J, Sillmann J and Alexander L 2022 Introduction to the special issue: Compound weather and climate events *Weather and Climate Extremes* **35** 100381

Zscheischler J, Westra S, van den Hurk B J J M, Seneviratne S I, Ward P J, Pitman A, AghaKouchak A, Bresch D N, Leonard M, Wahl T and Zhang X 2018 Future climate risk from compound events *Nat. Clim. Chang.* Online: https://doi.org/10.1038/s41558-018-0156-3

Supplementary Information for

Exposure to compound climate hazards transmitted via global agricultural trade networks

Patrick W. Keys[1,*], Elizabeth A. Barnes[1], Noah S. Diffenbaugh[2], Thomas W. Hertel[3], Uris L.C. Baldos[3], and Johanna Hedlund[4]

[1] Department of Atmospheric Science, Colorado State University
[2] Doerr School of Sustainability, Stanford University
[3] Department of Agricultural Economics, Purdue University
[4] Stockholm Environment Institute, Stockholm, Sweden

***Corresponding Author:** Patrick W. Keys

Email: patrick.keys@colostate.edu

This PDF file includes:

Text T1
Figures S1 to S15

Supplemental Text T1

For a single realization, for a single importer country "*M*", we define the fraction of *M*'s supply exposed to compound climate hazards according to the following workflow:

$$\text{fraction of } M\text{'s supply exposed} = \sum_{s \in S} t_{s,M} \left(\frac{\sum_{area} C \odot F \odot G_s}{\sum_{area} F \odot G_s} \right)$$

where

S = [set] all suppliers for country *M*

F = [lat/lon map] fraction of gridcell that is cropped

C = [lat/lon map] boolean mask of whether the gridcell is experiencing a compound climate hazard, taking irrigation into account for hot-dry conditions

$\mathbf{G_s}$ = [lat/lon map] boolean mask denoting the geographic domain of supplier *s* in **S**

t_s = [scalar] fraction of *M*'s supply that comes from supplier s

$\sum_{area}$ = area-weighted global sum

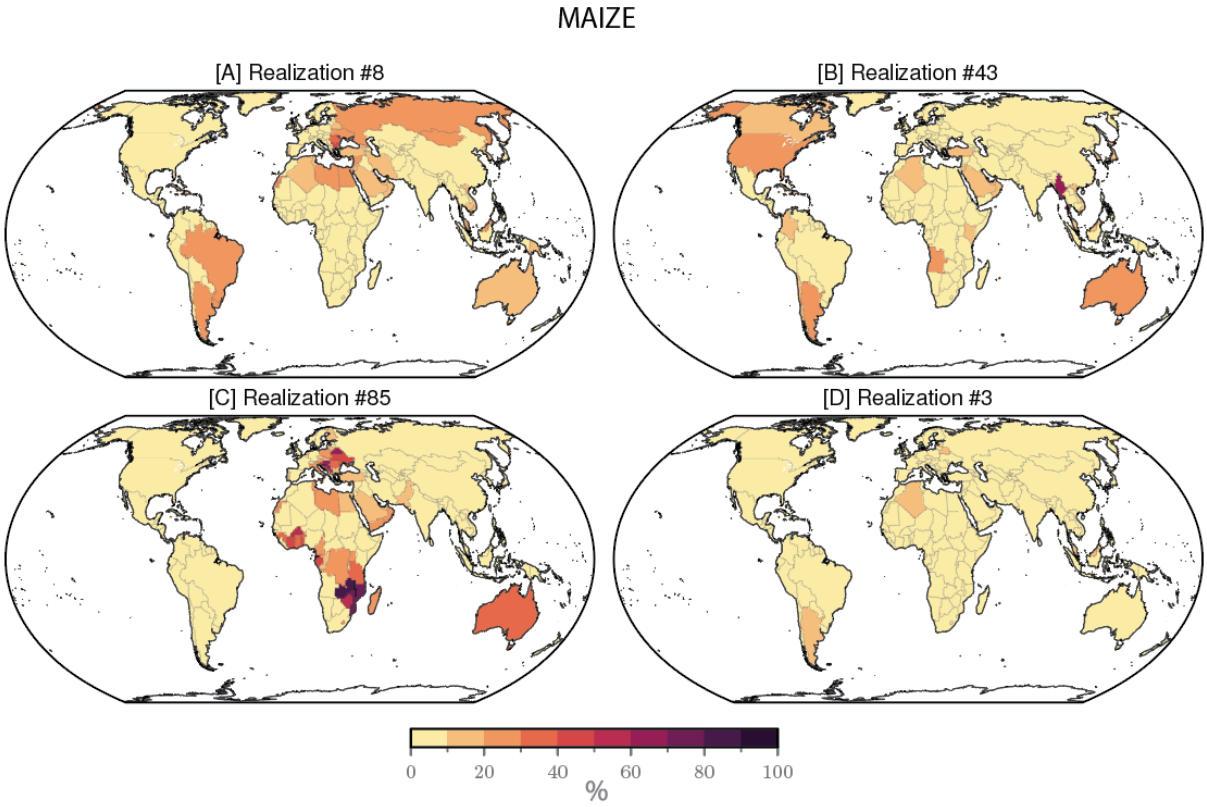

Figure S1. As in Figure 2 but for maize.

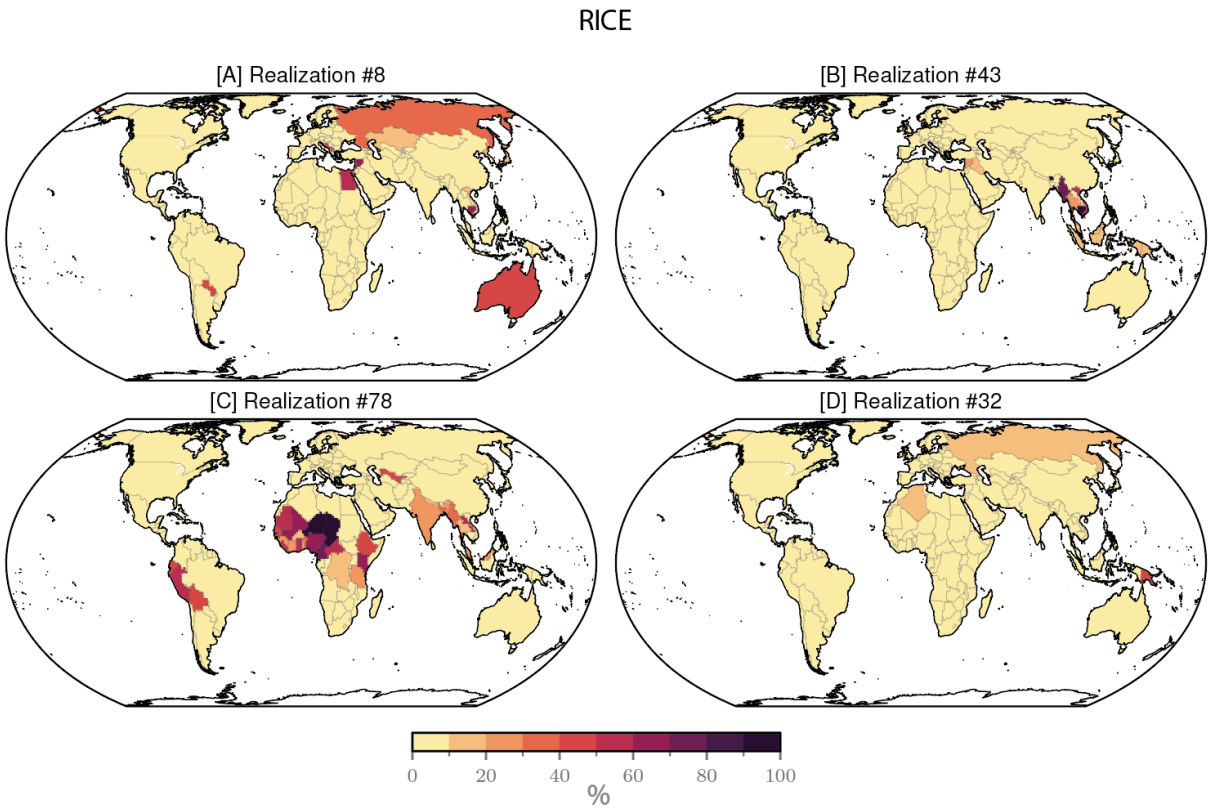

Figure S2. As in Figure 2 but for rice.

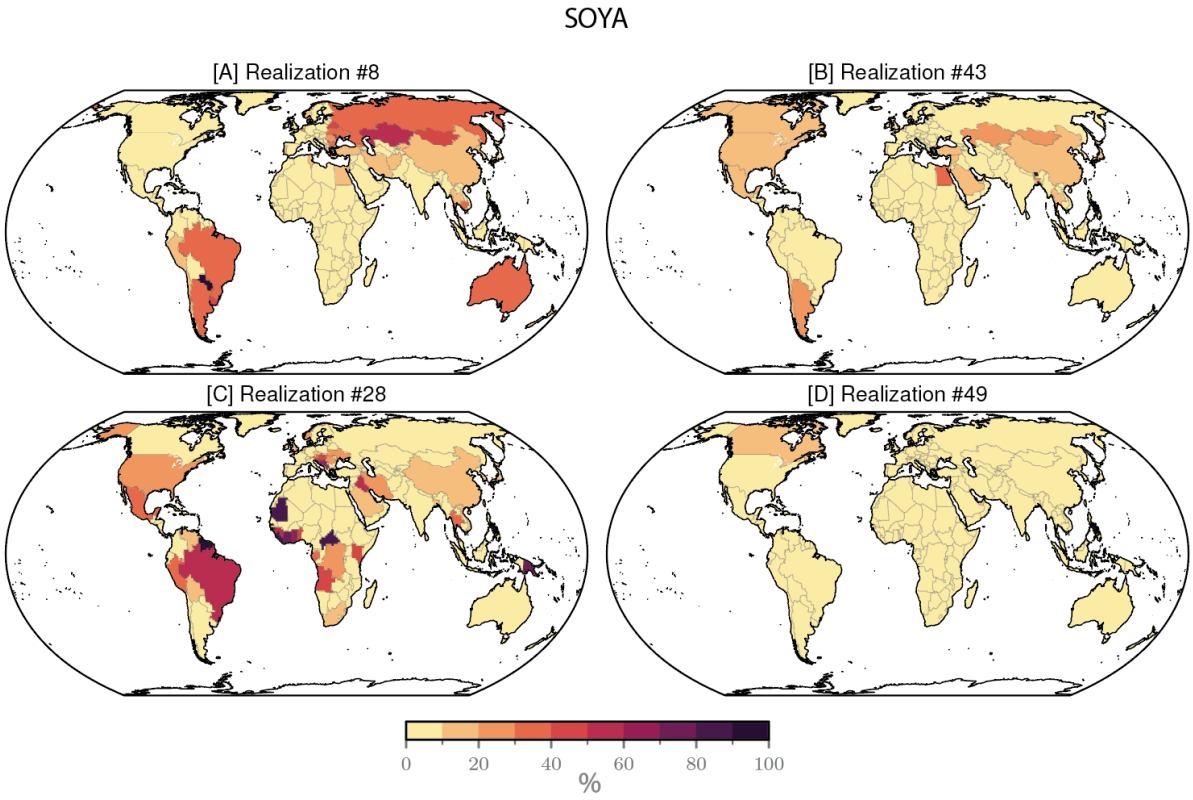

Figure S3. As in Figure 2 but for soya.

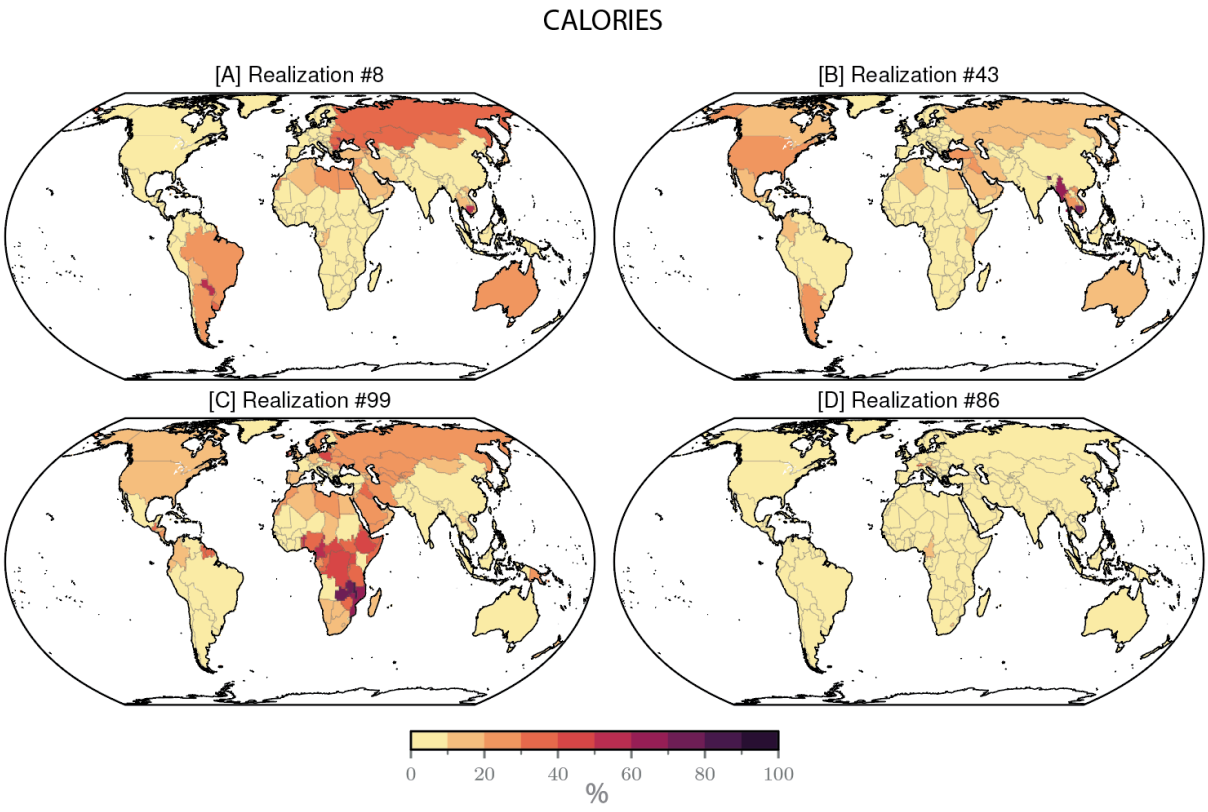

Figure S4. As in Figure 2 but for calories.

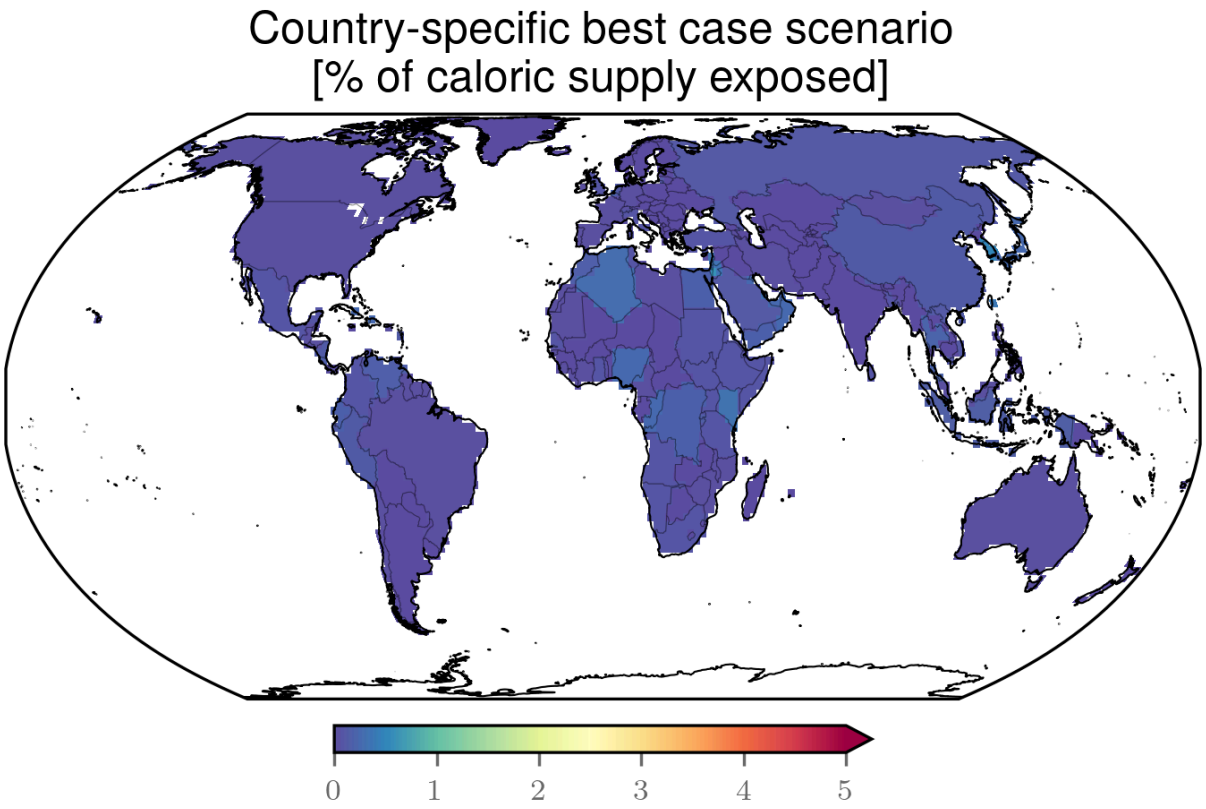

Figure S5. Country-specific best-case scenario for the percentage of caloric supply exposed to compound climate hazards.

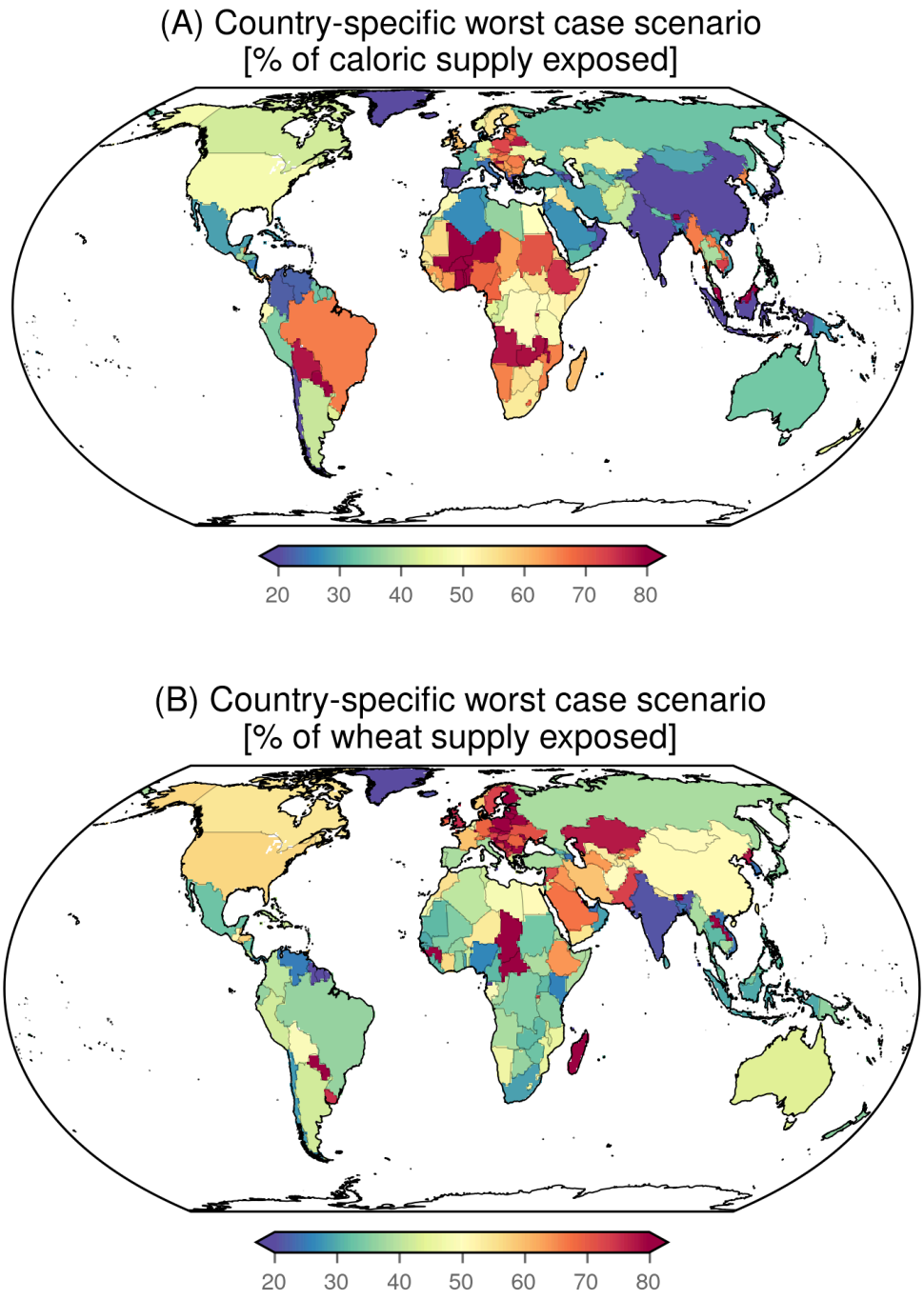

Figure S6. (A) Country-specific worst-case scenario for the percentage of caloric supply that is exposed to compound climate hazards. These values are also plotted as the colored shading of the dots in Figure 5. (B) As in (A) but for wheat.

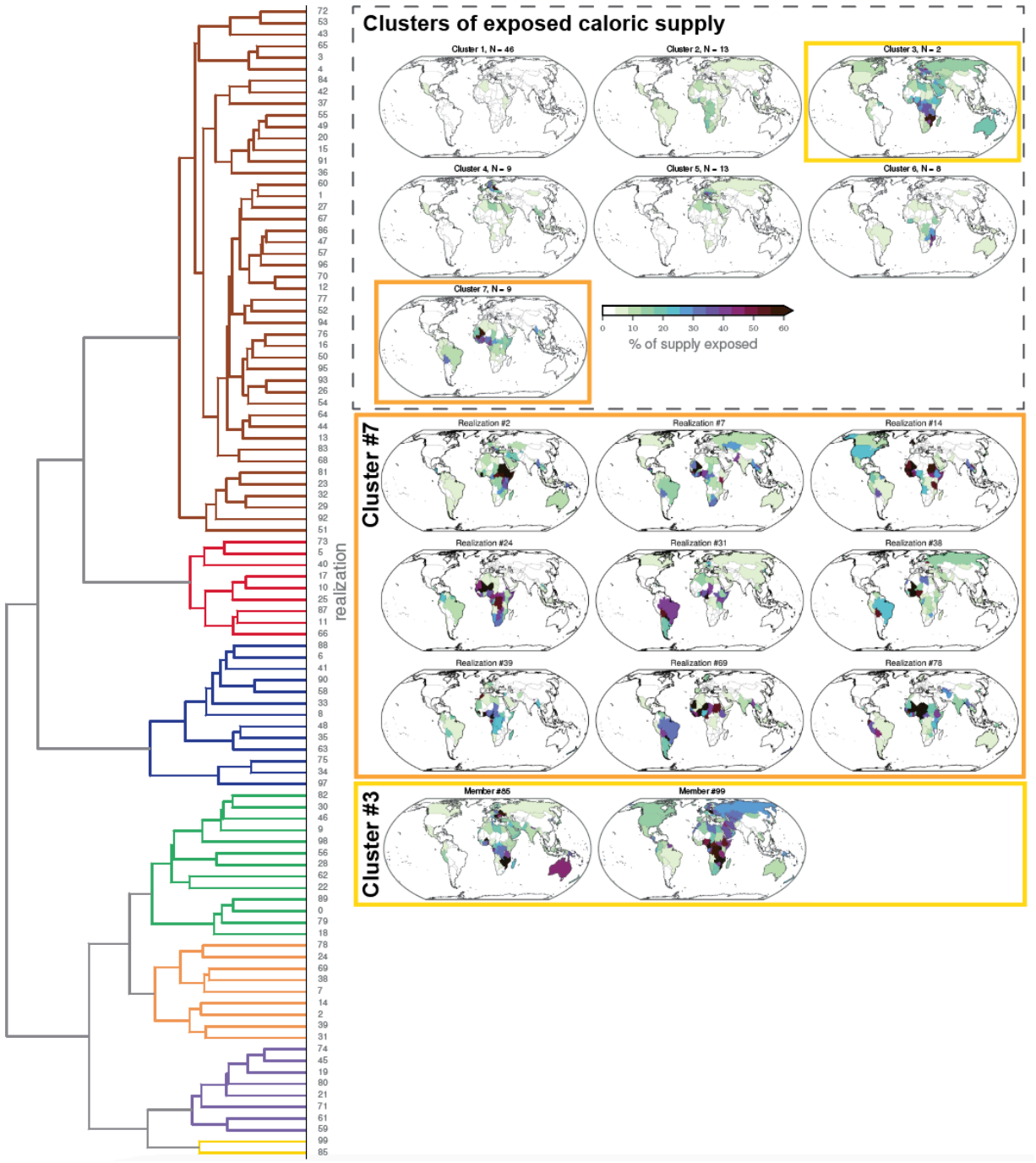

Figure S7. Visualization of the clustering of 100 realizations and the 7 mean clusters. Additional panels show the specific realizations that make up each of Clusters #7 and #3.

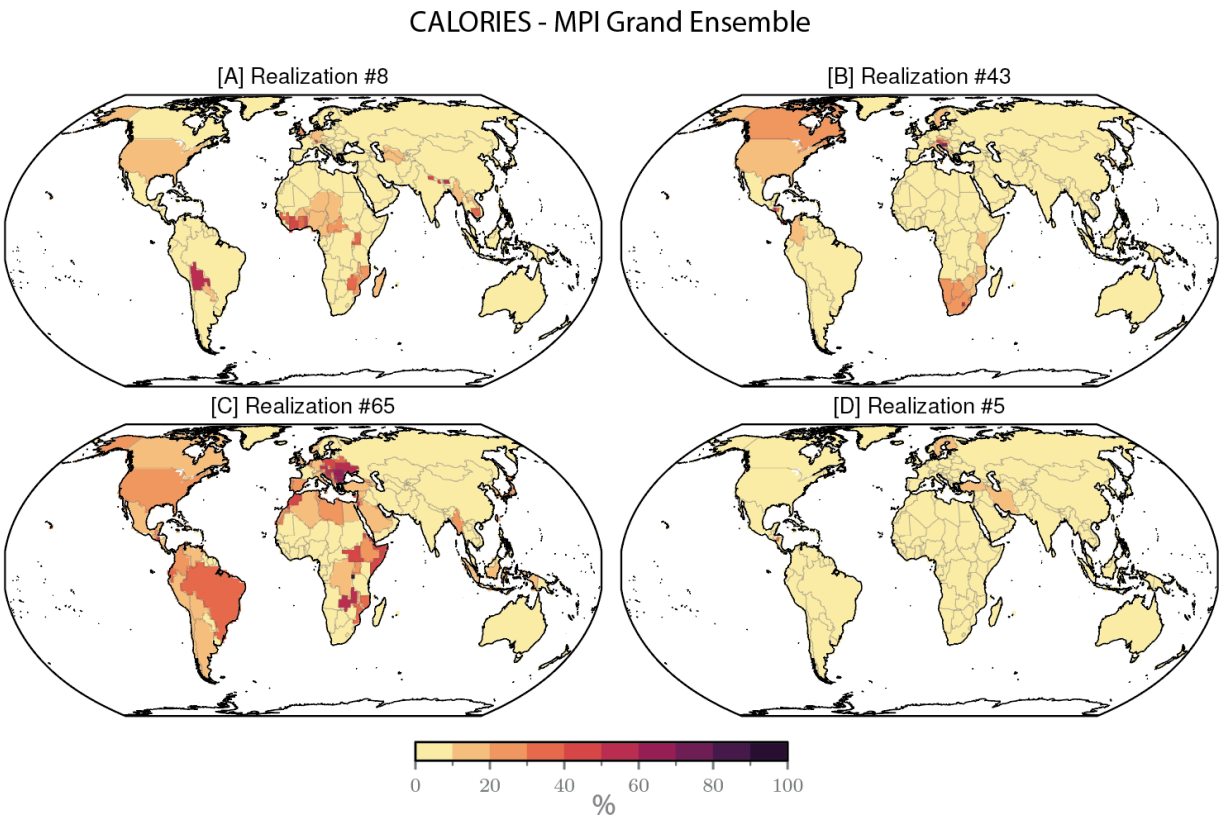

Figure S8. As in Figure 2 but using climate data from the MPI Grand Ensemble.

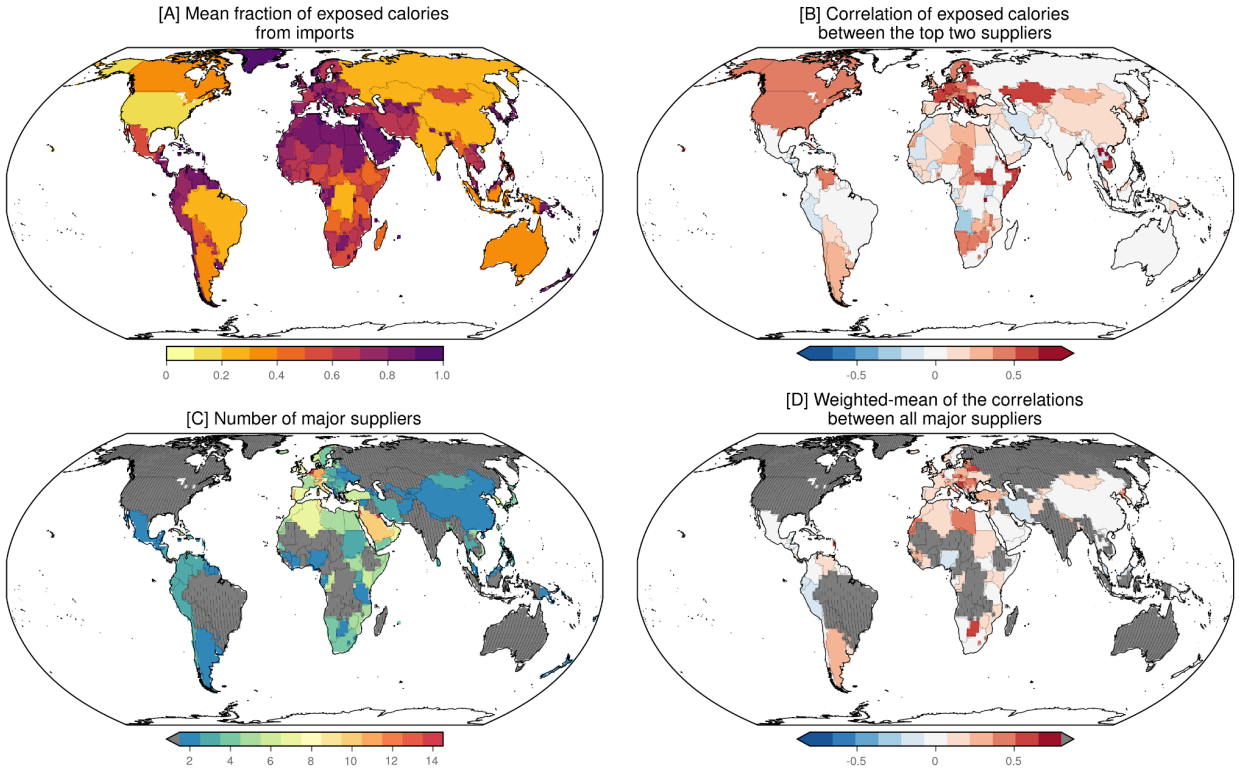

Figure S9. As in Figure 4 but using climate data from the MPI Grand Ensemble.

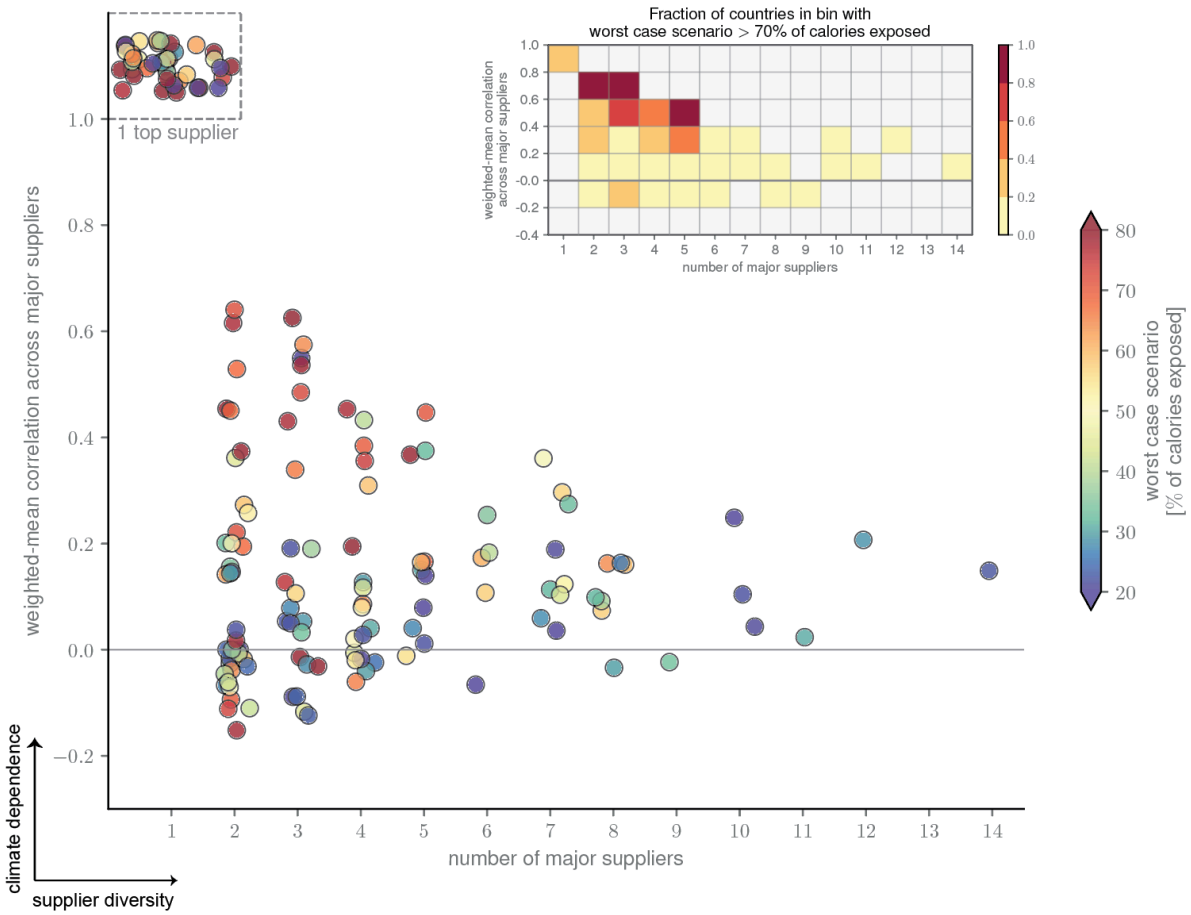

Figure S10. As in Figure 5 but using climate data from the MPI Grand Ensemble.

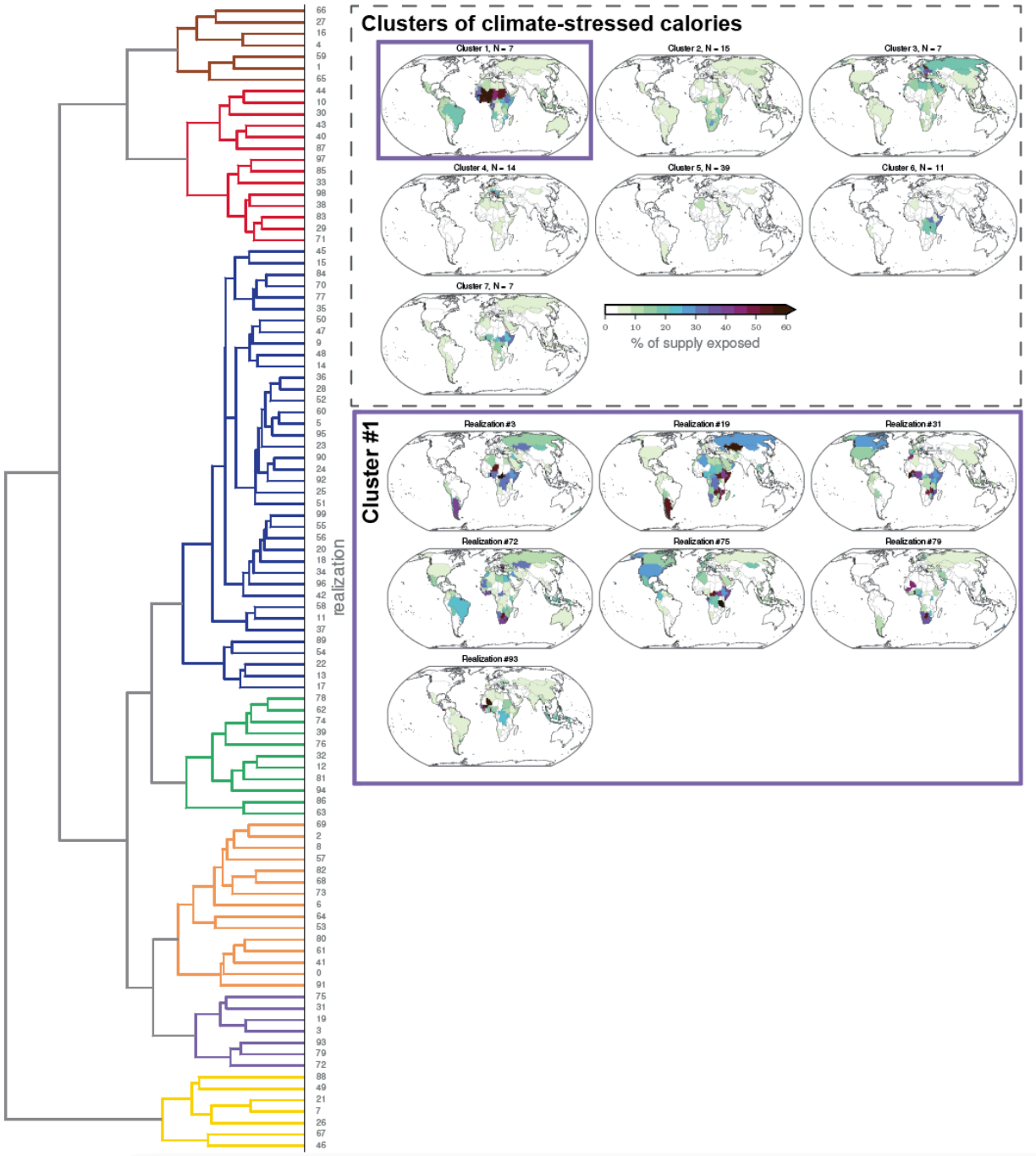

Figure S11. As in Supp. Fig. S7 but using climate data from the MPI Grand Ensemble.

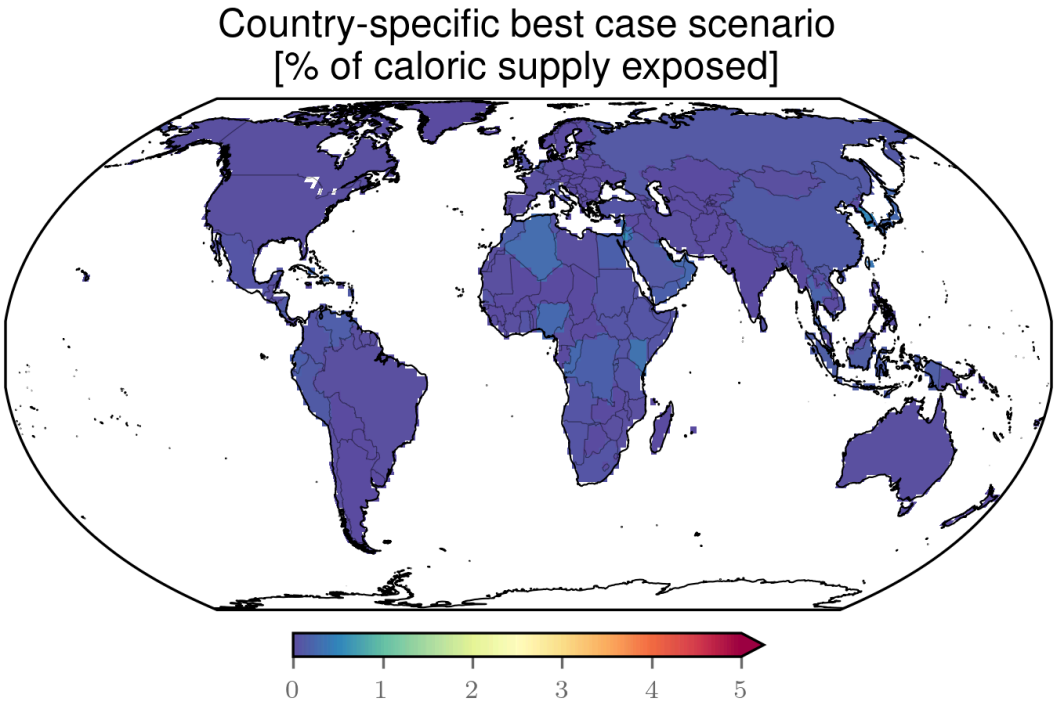

Figure S12. As in Supp. Fig. S5 but using climate data from the MPI Grand Ensemble.

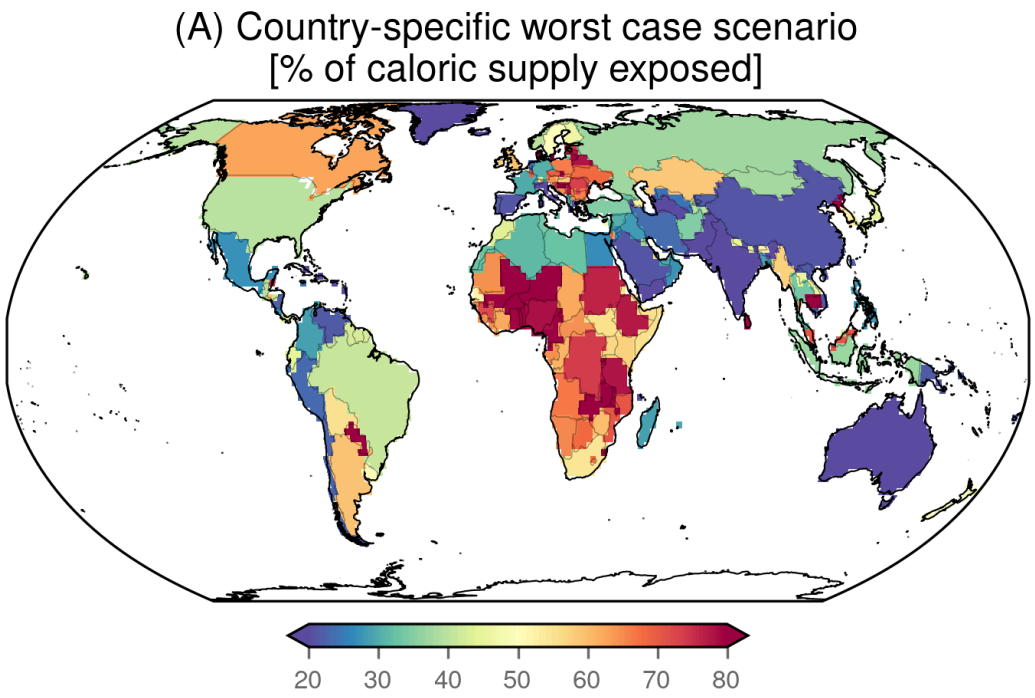

Figure S13. As in Supp. Fig. 6A but using climate data from the MPI Grand Ensemble.

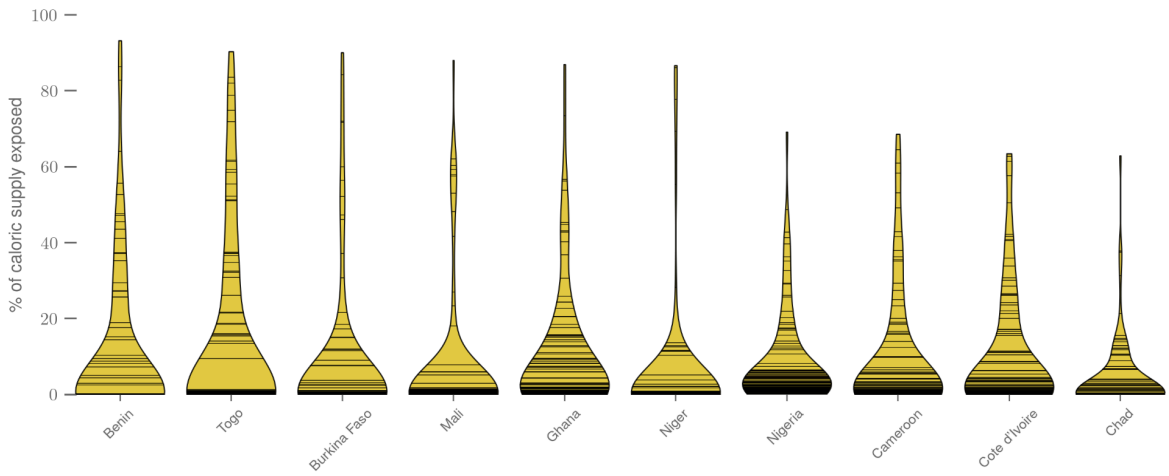

Figure S14. As in Fig. 3 but for caloric supply in select West African countries.

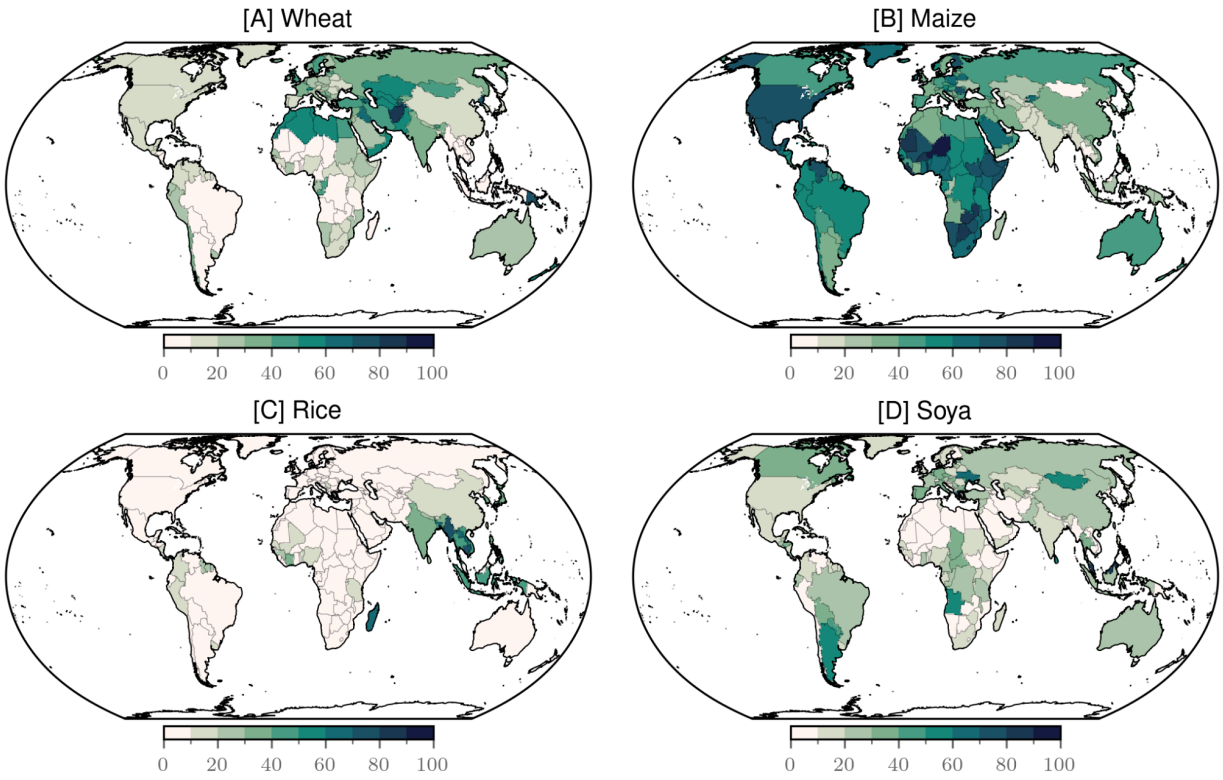

Figure S15. Percent of each country's caloric supply from each of the four crops considered here. As defined, the sum of panels A through D is 100%.